Investigation of the kinetic model equations

Sha Liu[*] and Chengwen Zhong[†]

National Key Laboratory of Science and Technology on Aerodynamic Design and Research, Northwestern Polytechnical University, Xi'an, Shaanxi 710072, China

(Received 4 September 2013; revised manuscript received 25 November 2013; published 12 March 2014)

Currently the Boltzmann equation and its model equations are widely used in numerical predictions for dilute gas flows. The nonlinear integro-differential Boltzmann equation is the fundamental equation in the kinetic theory of dilute monatomic gases. By replacing the nonlinear fivefold collision integral term by a nonlinear relaxation term, its model equations such as the famous Bhatnagar-Gross-Krook (BGK) equation are mathematically simple. Since the computational cost of solving model equations is much less than that of solving the full Boltzmann equation, the model equations are widely used in predicting rarefied flows, multiphase flows, chemical flows, and turbulent flows although their predictions are only qualitatively right for highly nonequilibrium flows in transitional regime. In this paper the differences between the Boltzmann equation and its model equations are investigated aiming at giving guidelines for the further development of kinetic models. By comparing the Boltzmann equation and its model equations using test cases with different nonequilibrium types, two factors (the information held by nonequilibrium moments and the different relaxation rates of high- and low-speed molecules) are found useful for adjusting the behaviors of modeled collision terms in kinetic regime. The usefulness of these two factors are confirmed by a generalized model collision term derived from a mathematical relation between the Boltzmann equation and BGK equation that is also derived in this paper. After the analysis of the difference between the Boltzmann equation and the BGK equation, an attempt at approximating the collision term is proposed.

DOI: 10.1103/PhysRevE.89.033306 PACS number(s): 02.60.Cb, 47.45.−n, 47.11.Df, 47.11.St

I. INTRODUCTION

Currently the Boltzmann equation and its model equations are widely used in the numerical prediction of dilute gas flows. The Boltzmann equation is the fundamental equation in the kinetic theory of dilute monatomic gases [1–4]. It is mathematically a nonlinear integro-differential equation. By replacing the nonlinear fivefold integral collision term by a modeled relaxation term, its model equations such as the famous Bhatnagar-Gross-Krook (BGK) equation [5,6] are mathematically simple. The collision term of Boltzmann equation is based on microscopic molecule collisions, while the model collision term is based on the result of all collisions that the distribution has the trend towards equilibrium. Since the computational cost of solving model equations is much less than that of solving the full Boltzmann equation, the model equations are widely used in predicting rarefied flows [7–11], multiphase flows [12–16], chemically reacting flows [17–20], and turbulent flows [21–25] although their predictions for highly nonequilibrium flows are only qualitatively right in transitional regime since they filter out the information of detailed collision process.

At the present stage, two classes of numerical methods based on gas kinetic theory are used for predicting the dilute gas flows, i.e., statistical and deterministic. The statistical method, represented by the direct simulation Monte Carlo (DSMC) method [26–30], uses probabilistic simulation to solve the Boltzmann equation for finite Knudsen number dilute gas flows. The deterministic method, represented by the so-called discrete velocity methods (DVM) or discrete ordinate method (DOM) [31–35], solves the governing equation by using regular discretization of particle velocity. Besides the above approaches, many other methods, such as the finite difference [36], spectral [37–39], lattice-gas automata [40,41], and lattice Boltzmann method [13,14], have been developed as well. In order to simplify the numerical schemes for the Boltzmann equation, both statistical and deterministic methods use an operator splitting approach, such as decoupling the transport and collision process into a collisionless free transport and particle collision. Due to the decoupled processes, the cell size and time step in the operator splitting methods are generally limited by the mean free path and the mean collision time, respectively, which makes these methods prohibitively expensive in the transition and continuum flow regimes. The operator splitting is originally used to avoid the mathematical difficulty in dealing with the nonlinear integro-differential Boltzmann equation. When using the kinetic collision models instead of the quadratic collision integral of the Boltzmann equation, there is no need to use the operator splitting method and consequently be limited by the mean free path and collision time. With the coupled transport and collision process, a unified gas kinetic scheme (UGKS) has been developed and achieved successes from the continuum flow regime to the rarefied flow regime [7–9,11,42]. For the calculation of numerical flux, the coupled transport and collision process is more physical and more precise than the upwind scheme used in the original DVM [11]. After necessary modification, the UGKS is used as a numerical solver in this paper.

In this paper the differences between the Boltzmann equation and its model equations are investigated aiming at giving guidelines for improving the accuracy of model equations in a kinetic regime. First, the kinetic model equations and the Boltzmann equation are compared numerically in a plane shock structure test case and a homogenous relaxation

[*]shaliu@mail.nwpu.edu.cn

[†]Corresponding author: zhongcw@nwpu.edu.cn

test case in kinetic regime, where the distribution functions are far from equilibrium and the deviations of kinetic model equations are expected to be large. From these tests, the information held by nonequilibrium moments and the different relaxation rates of high- and low-speed molecules are found useful in adjusting the behaviors of model collision terms. Then a mathematical relationship between the BGK equation and the Boltzmann equation is derived, in which the Boltzmann collision integral is split into a BGK relaxation term and a non-BGK deviation. By using this relationship, a generalized relaxation term can be also constructed. The usefulness of the information of nonequilibrium moments and the different relaxation rate is confirmed by the generalized relaxation term. Finally, after the analysis of non-BGK deviation, an attempt at calculating the collision integral is proposed where the integrals are constructed using simple patterns.

This paper is organized as follows. The Boltzmann equation and the kinetic model equations are introduced in Sec. II. Section III is a brief introduction of a unified gas kinetic scheme. Section IV is the numerical comparisons of kinetic model equations and Boltzmann equation along with the analysis of them. Section V includes the derivation of the relationship between the BGK equation and Boltzmann equation and the construction of the generalized relaxation term. Section VI includes the analysis of the deviation integral and a method for approximating the collision integral. The discussion and concluding remarks are drawn in the final section.

II. BOLTZMANN EQUATION AND KINETIC MODEL EQUATIONS

A. Boltzmann equation

In the kinetic theory of dilute gases, the state of a system of particles is determined by a distribution function $f(\boldsymbol{x},\boldsymbol{\xi},t)$, which depends on the location $\boldsymbol{x}$, the particle velocity $\boldsymbol{\xi}$, and time t. The distribution function defines the possibility density that a particle presents at $(\boldsymbol{x},\boldsymbol{\xi})$ in phase space at time t. The time evolution of the distribution function is governed by the Boltzmann equation

$$\frac{\partial f}{\partial t}+\boldsymbol{\xi}\cdot\nabla_{\boldsymbol{x}} f = I(f,f). \tag{1}$$

The left-hand side (LHS) of Eq. (1) is the transport term, which is the time derivative of f in the Lagrangian coordinate system and is also called a substantial derivative in the field of fluid dynamics. The right-hand side (RHS) of Eq. (1) is the collision term, which describes the binary collision between particles. For elastic collisions of monatomic dilute gases, it has the form

$$I(\boldsymbol{\xi}) = \int_{R^3}\int_{S^2}[f(\boldsymbol{\xi}_1')f(\boldsymbol{\xi}') - f(\boldsymbol{\xi}_1)f(\boldsymbol{\xi}])B(v,\boldsymbol{\Omega})d\boldsymbol{\Omega}\,d\boldsymbol{\xi}_1, \tag{2}$$

where $v=|\boldsymbol{\xi}-\boldsymbol{\xi}_1|$ is the relative velocity of colliding particles, $B(v,\boldsymbol{\xi})$ is the collision kernel, and $\boldsymbol{\Omega}$ is the solid angle. The postcollision velocities $\boldsymbol{\xi}_1'$ and $\boldsymbol{\xi}'$ are determined by the precollision velocities $\boldsymbol{\xi}$ and $\boldsymbol{\xi}_1$ with the aid of classical conservation laws and the geometric information of solid angle $\boldsymbol{\Omega}$.

The collision integral can be split into two integrals called the depleting term and the replenishment term representing the rate of losing and regaining molecules, respectively:

$$I(\boldsymbol{\xi}) = -\int_{R^3}\int_{S^2} f(\boldsymbol{\xi}_1)f(\boldsymbol{\xi})B(v,\boldsymbol{\Omega})d\Omega d\boldsymbol{\xi}_1 + \int_{R^3}\int_{S^2} f(\boldsymbol{\xi}_1')f(\boldsymbol{\xi}')B(v,\boldsymbol{\Omega})d\boldsymbol{\Omega}\,d\boldsymbol{\xi}_1. \tag{3}$$

In the depleting term, $f(\boldsymbol{\xi})$ can be written on the outside of the integral, and the rest of the collision integral is the collision frequency ν, which is defined as

$$\nu = \int_{R^3}\int_{S^2} f(\boldsymbol{\xi}_1)B(v,\boldsymbol{\Omega})d\boldsymbol{\Omega}\,d\boldsymbol{\xi}_1. \tag{4}$$

Denote the inverse collision integral by R for replenishment, and the Boltzmann equation can be written as

$$\frac{\partial f}{\partial t}+\boldsymbol{\xi}\cdot\nabla_{\boldsymbol{x}} f = R-\nu(\boldsymbol{\xi})f(\boldsymbol{\xi}). \tag{5}$$

B. The kinetic model equations

As a model equation of the fundamental Boltzmann equation, the BGK equation [5] has a relaxation collision term and is robust for a wide range of numerical schemes. The BGK equation is in the form

$$\frac{\partial f}{\partial t}+\boldsymbol{\xi}\cdot\nabla_{\boldsymbol{x}} f = \nu_{\mathrm{BGK}}(\boldsymbol{\xi})[g(\boldsymbol{\xi})-f(\boldsymbol{\xi})], \tag{6}$$

where ν_{BGK} is the relaxation rate, which is determined by the viscosity and is on the same order of a mean collision frequency. g is the local equilibrium state given as

$$g(\boldsymbol{\xi}) = n\left(\frac{m}{2\pi kT}\right)^{3/2}\exp\left(-\frac{m}{2kT}|\boldsymbol{\xi}-\boldsymbol{u}|^2\right), \tag{7}$$

where k is the Boltzmann constant, m is the particle mass, and n, $\boldsymbol{u}$, and T are the particle number, macroscopic velocity, and temperature, respectively. These macroscopic variables depend on the local distribution function:

$$\begin{aligned} n &= \int_{R^3} f(\boldsymbol{\xi})d\boldsymbol{\xi},\\ \boldsymbol{u} &= \frac{1}{n}\int_{R^3}\boldsymbol{\xi} f(\boldsymbol{\xi})d\boldsymbol{\xi},\\ T &= \frac{1}{nk}\int_{R^3}|\boldsymbol{\xi}-\boldsymbol{u}|^2 f(\boldsymbol{\xi})d\boldsymbol{\xi}. \end{aligned} \tag{8}$$

The collision term of the BGK equation describes the trend of distribution toward equilibrium. Compared with the Boltzmann collision term, the BGK collision term filters out the detailed information of the collision process.

According to gas kinetic theory, the BGK model corresponds to an unchangeable unit Prandtl number [6], but the Prandtl number for monatomic gases is about 2/3. To get a right Prandtl number, many statistical models have been proposed, such as the ES-BGK model [43], the Shakhov model [44], and the $\nu(c)$-BGK model [45,46]. The ES-BGK and Shakhov models replace the Maxwellian state in the BGK collision term with new ones: the ES-BGK model holds that the molecules which emerge from collisions have some memory of their original states, and a new state is constructed by a

weighted average of the original state and equilibrium state; in the Shakhov model, the new equilibrium state is represented by a third order Hermitian expansion whose zero order term is a Maxwellian state. Being different from the ES-BGK and the Shakhov models, the $\nu(c)$-BGK model replaced the relaxation rate, which is independent of velocity in the BGK relaxation term, with a velocity-dependent one which better fits the physical reality. Although the ideas of these models are totally different, they all give a right Prandtl number, while, due to different ways of approximating the Boltzmann collision term, their relaxation behaviors are different.

1. ES-BGK model

In ES-BGK model [43], the Maxwellian equilibrium distribution g is replaced by a Gaussian distribution $g_{\rm es}$. The temperature T in the BGK equation, which is a second order moment of the distribution function, is extended to a second order moment tensor ${T^{\rm es}}_{ij}$. The tensor leads to a anisotropic temperature which introduces certain amount of nonequilibrium into the new equilibrium state $g_{\rm es}$. The Gaussian equilibrium state is written as

$$g_{\rm es} = n\left(\frac{m}{2\pi k}\right)^{3/2}\sqrt{\frac{1}{\det({T^{\rm es}}_{ij})}}\exp\left(-\frac{m}{2k}c_i{{T^{\rm es}}_{ij}}^{-1}c_j\right), \quad (9)$$

where $\boldsymbol{c}$ is the peculiar velocity $\boldsymbol{c} = \boldsymbol{\xi} - \boldsymbol{u}$, and the temperature tensor is defined as

$$\begin{aligned}{T^{\rm es}}_{ij} &= \frac{1}{nk}\int_{R^3} c_i c_j[(1-b)g + bf]\,d\boldsymbol{\xi} \\ &= \frac{(1-b)}{nk}\delta_{ij}P + \frac{b}{nk}p_{ij}, \end{aligned} \quad (10)$$

where P is the pressure and p_{ij} is the stress tensor. It should be noted that relaxation rate of ES-BGK is different from that of the BGK. When applying a second order Chapman-Enskog expansion to the ES-BGK model, it has two free parameters b and ν to make the obtained viscosity coefficient and heat conduction coefficient coincide with the real ones. So b is set to be $1 - 1/\Pr$, and $\nu_{\rm es}$ is set to be $\Pr p/\nu = \Pr \nu_{\rm BGK}$.

The $\nu_{\rm BGK}g$ term in the BGK relaxation term can be related to the replenishment term R in the full Boltzmann equation by replacing f, the integrand of the quadratic integral, by g. When the replenishment term is written as $\nu_{\rm BGK}g$, it means that the distribution of particles emerging from collisions is Maxwellian, or after collision, the distribution of particles changes from nonequilibrium to equilibrium accidently. Obviously the physical reality is that after 10 or even more mean collision times, a high nonequilibrium state can approach its equilibrium. This reality will also be shown phenomenally in Sec. IV. In Holway's paper [43], it is believed that postcollision particles should have some memories of their precollision states. One of the important and apparent features of the nonequilibrium precollision state is its spherical asymmetry in the shape of the distribution function.

2. Shakhov model

In the Shakhov model [44] for pseudo-Maxwell molecules, a new equilibrium state is constructed by using a multidimensional Hermitian expansion around the Maxwellian equilibrium state, which was first used by the moment method solution of the Boltzmann equation [47]. The Hermitian series are truncated at the third order aiming to restore the third order moment, which is the heat flux. Then the coefficients of Hermitian series are chosen by making the Shakhov collision term fulfill the mass, momentum, and energy conservation laws, along with the right relaxation rate of heat flux. The new equilibrium state $g_{\rm Shakhov}$ has the following form:

$$\begin{aligned} g_{\rm Shakhov} = n\left(\frac{m}{2\pi kT}\right)^{3/2}\exp\left(-\frac{mc^2}{2kT}\right) \\ \times\left[1 + \frac{1-\Pr}{5}\frac{mq_i c_i}{kTP}\left(\frac{mc^2}{kT} - 5\right)\right], \end{aligned} \quad (11)$$

where the heat flux q_i can be expressed in the form of

$$q_i = \frac{m}{2}\int_{R^3} c_i c^2 f\,d\boldsymbol{\xi}. \quad (12)$$

The Shakhov collision term approximates the Boltzmann collision term in a way that makes its relaxation rates of low order moments coincide to that of the Boltzmann collision term. Theoretically, for a pseudo-Maxwell molecule, a higher order Hermitian series could be used, which may make the collision term more accurate.

3. $\nu(c)$-BGK model

The $\nu(c)$-BGK model uses a velocity-dependent collision frequency, which is based on the observation of particle collisions. This collision frequency can be assumed to be any function with two free parameters which can be determined by experimental values of viscosity and thermal conductivity. In Refs. [45,46], these functions are expressed in the form of polynomials of C, which is a nondimensional peculiar velocity $|\boldsymbol{c}|/\sqrt{2RT}$. A possible expression of $\nu(c)$ is formulated as

$$\nu = a(1 + \gamma C^2)\frac{P}{\mu}, \quad (13)$$

with two coefficients $a = 0.0268351$ and $\gamma = 14.2724$. More polynomials can be found in Ref. [45]. Though the velocity-dependent collision frequency yields a correct Prandtl number, the relaxation process of the $\nu(c)$-BGK model differs significantly from that of the BGK model. This difference will be illustrated in Sec. IV. So the function of the velocity-dependent collision frequency should be chosen carefully in order to approximate the Boltzmann collision term well.

III. THE UNIFIED GAS KINETIC SCHEME

The kinetic model equations are solved by the unified gas kinetic scheme in this paper. The UGKS is a multiscale method with coupled transport and collision processes [7]. The mathematical realization of coupled processes is through the integral solution of the kinetic model equation, which is used as a gas evolution model at the cell interface. Since the integral solution includes both kinetic scale and hydrodynamic scale mechanisms, it leads to an automate recovering of kinetic scale and hydrodynamic scale solutions. Due to the coupled evolution process, the cell size and time step are not limited by the mean free path and the mean collision time, respectively.

The UGKS can be classified into a finite volume method. The physical space is divided into finite control volume $V_{i,j,k}$. The temporal discretization is denoted by t^n for the nth time step. After integrating the kinetic model equation over a certain control volume and time interval, the finite volume form can be written as

$$f_{i,j,k}^{n+1} = f^n + \frac{1}{V}\int_{t^n}^{t^{n+1}} \oint_{\partial V} \boldsymbol{\xi} f_{cf} \cdot d\boldsymbol{S}\, dt + \frac{1}{V}\int_{t^n}^{t^{n+1}} \frac{g^+_{i,j,k} - f_{i,j,k}}{\tau}\, dt, \tag{14}$$

where $f_{i,j,k}$ is a cell-averaged value in $V_{i,j,k}$, g^+, and τ is the equilibrium state and mean relaxation time, $f_{cf} = f(\boldsymbol{x}_{cf},\boldsymbol{\xi},t)$ is the evolution of distribution at the cell interface, and $\boldsymbol{x}_{cf}$ is the center of the cell interface. The most important feature of UGKS is the construction of f_{cf} in the following form:

$$f_{cf}(\boldsymbol{\xi},t) = \frac{1}{\tau}\int_{t^n}^{t} g^+(\boldsymbol{x}',\boldsymbol{\xi},t')e^{-(t-t')/\tau}\, dt' + e^{-(t-t^n)/\tau} f(\boldsymbol{x}_0,\boldsymbol{\xi},t_n), \tag{15}$$

where $\boldsymbol{x}' = \boldsymbol{x}_{cf} - \boldsymbol{\xi}\cdot(t-t')$ is the particle trajectory varying with time t' from t^n to t, and $\boldsymbol{x}_0 = \boldsymbol{x}_{cf} - \boldsymbol{\xi}\cdot(t-t_n)$ is the original position (at t_n) of the particle that arrives at $\boldsymbol{x}_{cf}$ at t.

The analytical solution describes the traveling of a cluster of molecules. When traveling on the route, $vf(\boldsymbol{x}',\boldsymbol{\xi},t')dt$ molecules among them collide with other molecules and leave the route, while $[vg^+(\boldsymbol{x}',\boldsymbol{\xi},t')dt]$ molecules, which are not on the route originally, replenish this cluster of molecules through certain intermolecular collisions. At the final time t, there are $e^{-(t-t^n)/\tau}$ of the original amount of molecules that are left over, and $\frac{1}{\tau}\int_{t^n}^{t} g^+(\boldsymbol{x}',\boldsymbol{\xi},t')e^{-(t-t')/\tau}\, dt'$ molecules replenish this cluster from other routes. The integral solution is actually a gas evolution model which describes coupled transportation and collision. Compared with the upwind treatment used in the operator splitting method where only the transportation is considered, the integral solution is more physical and is without the extra viscosity associated with the upwind treatment [11].

Multiply Eq. (14) by $\boldsymbol{\psi} = (1,\boldsymbol{\xi},|\boldsymbol{\xi}|^2)$ and integrate it over the whole velocity space; then the corresponding evolution functions for macroscopic properties $\boldsymbol{W} = (\rho,\rho\boldsymbol{u},\rho e)$ can be obtained in the form

$$\mathbf{W}_{i,j,k}^{n+1} = \mathbf{W}_{i,j,k}^{n} + \frac{1}{V}\int_{t^n}^{t^{n+1}} \oint_{\partial V} \boldsymbol{F}\cdot d\boldsymbol{S}\, dt + , \tag{16}$$

where the flux term $\boldsymbol{F}$ is defined as

$$\boldsymbol{F} = \int_{R^3} \boldsymbol{\xi}\boldsymbol{\psi} f_{cf}\, d\boldsymbol{\xi}. \tag{17}$$

To obtain the detailed distribution functions, which is important for the prediction of rarefied gas flows, a discrete particle velocity space is used in UGKS. The discrete distribution function $f_{i,j,k,l,m,n}$ is defined as the average value in certain discrete subspace:

$$f_{i,j,k,l,m,n}^{n} = \frac{1}{\Delta\xi_l\Delta\xi_m\Delta\xi_n V_{i,j,k}}\int_{V_{i,j,k}}\int_{W_{l,m,n}} f(\boldsymbol{x},\boldsymbol{\xi},t^n)\, d\boldsymbol{\xi}\, dV, \tag{18}$$

where the velocity space is divided into cubic elements centered at ξ_l,ξ_m,ξ_n with span $\Delta\xi_l,\Delta\xi_m,\Delta\xi_n$.

To discrete the collision term efficiently, the implicit form is used as

$$\frac{\Delta t}{2}\left(\frac{g_{i,j,k,l,m,n}^{n+1} - f_{i,j,k,l,m,n}^{n+1}}{\tau_{i,j,k}^{n+1}} + \frac{g_{i,j,k,l,m,n}^{n} - f_{i,j,k,l,m,n}^{n}}{\tau_{i,j,k}^{n}}\right). \tag{19}$$

To determine the equilibrium distribution g^{n+1} in this implicit form of collision term, the conservative macroscopic properties at the $(n+1)$-th time step should be updated using Eq. (16) first. For Shakhov and ES-BGK equations, nonconservative macroscopic properties, such as the stress tensor and heat flux, should also be updated. In this paper, the stress tensor $p_{\alpha\beta}$ and heat flux q_α are updated using

$$p_{\alpha\beta}{}_{i,j,k}^{n+1} = p_{\alpha\beta}{}_{i,j,k}^{n} + \frac{1}{V}\int_{t^n}^{t^{n+1}} \oint_{\partial V}\int_{R^3} \boldsymbol{\xi} c_\alpha c_\beta f_{cf}\, d\boldsymbol{\xi}\cdot d\boldsymbol{S}\, dt + \frac{1}{V_{i,j,k}}\frac{\Delta t}{2}\left(\frac{p_{\alpha\beta}{}_{i,j,k}^{n+1} - P_{i,j,k}^{n+1}\delta_{\alpha\beta}}{\tau_{i,j,k}^{n+1}} + \frac{p_{\alpha\beta}{}_{i,j,k}^{n} - P_{i,j,k}^{n}\delta_{\alpha\beta}}{\tau_{i,j,k}^{n}}\right),$$
$$q_{\alpha}{}_{i,j,k}^{n+1} = q_{\alpha}{}_{i,j,k}^{n} + \frac{1}{2V}\int_{t^n}^{t^{n+1}} \oint_{\partial V}\int_{R^3} \boldsymbol{\xi} c_\alpha c^2 f_{cf}\, d\boldsymbol{\xi}\cdot d\boldsymbol{S}\, dt + \frac{1}{V_{i,j,k}}\frac{\Delta t}{2}\left(\frac{q_{\alpha}{}_{i,j,k}^{n+1}}{\tau_{i,j,k}^{n+1}} + \frac{q_{\alpha}{}_{i,j,k}^{n}}{\tau_{i,j,k}^{n}}\right). \tag{20}$$

With the information on macrovariables at the $(n+1)$-th time step, the collision time τ can be calculated using $\tau = \mu(T)/P$. Thus the final numerical governing equation of UGKS is

$$f_{i,j,k,l,m,n}^{n+1} = f_{i,j,k,l,m,n}^{n} + \frac{1}{V}\int_{t^n}^{t^{n+1}} \oint_{\partial V}\int_{R^3} \boldsymbol{\xi} f_{cf}\, d\boldsymbol{\xi}\cdot d\boldsymbol{S}\, dt + \frac{1}{V_{i,j,k}}\frac{\Delta t}{2}\left(\frac{g_{i,j,k,l,m,n}^{n+1} - f_{i,j,k,l,m,n}^{n+1}}{\tau_{i,j,k}^{n+1}} + \frac{g_{i,j,k,l,m,n}^{n} - f_{i,j,k,l,m,n}^{n}}{\tau_{i,j,k}^{n}}\right). \tag{21}$$

IV. COMPARISON OF BOLTZMANN EQUATION AND KINETIC MODEL EQUATIONS

In the scope of numerical predictions, the validity of the kinetic model equation can be described as follows. In the continuum regime, the distribution functions are often not far from equilibrium, and the shock wave is treated as a discontinuity from the macroperspective. Since the deviation of the model collision term is very small in this situation, the model equations can be used. In a free molecule regime, since the weight of an interparticle collision is much lower than that of the collision between the particle and a solid wall, choosing

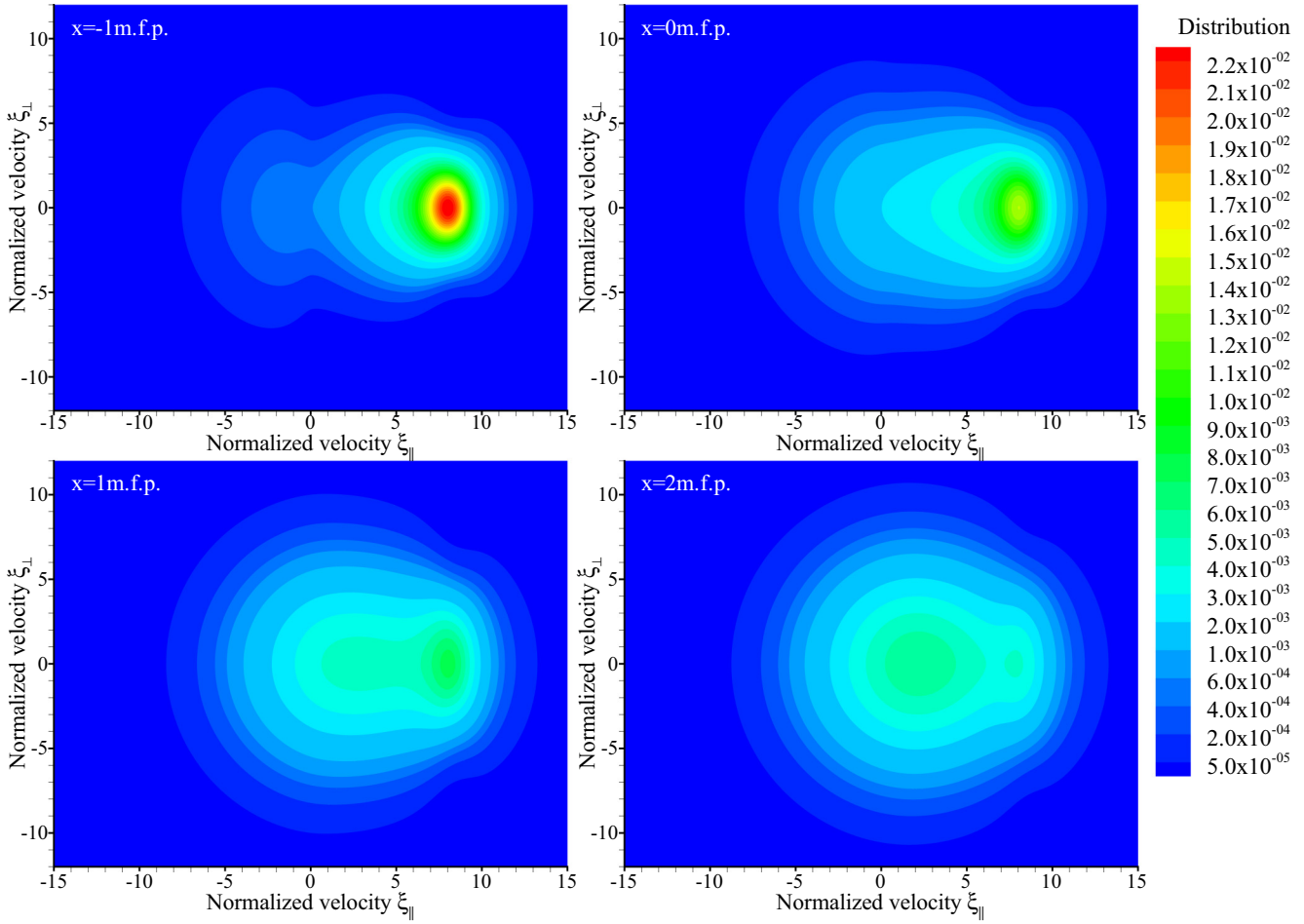

FIG. 1. (Color online) The distribution function in the shock.

the model collision term or the Boltzmann collision term for numerical prediction makes no great difference. Thus the model equation can also be used, although the model collision term may deviate significantly from the Boltzmann collision term in this situation. In a transitional regime, the deviation of the model collision term cannot be avoided since the weight of the interparticle collision is equivalent to that of the collision between the particle and solid wall. Thus the model equation can only give qualitatively right results in this regime. In this section a shock wave structure case and a homogenous relaxation case are carried out trying to find the qualitative difference between the model equations and the Boltzmann equation along with some practical principles for improving the accuracy of model equations in the transition flow regime.

A. The shock wave structure case

The normal shock wave, when measured using macroscopic instruments, is a discontinuity where the physical properties change accidently before and after the shock wave. On the other hand, from the view of microscopic scale, the profiles of physical properties in the discontinuous shock are actually smooth. Molecules in the shock are mixed with the molecules before the shock (supersonic and hypersonic, low temperature) and after the shock (subsonic, high temperature). Thus when the Mach number is high, the distribution function is approximately bimodal, with a low speed and wide stretched part and a high speed and narrow part. Figure 1 illustrates the distribution function in the Mach 8 shock wave on a $\xi_\parallel\xi_\perp$ plane, where $\parallel$ represents the stream direction and $\perp$ represents the perpendicular direction. Since the equilibrium Maxwellian state is monocentric, the bimodal distribution shows great nonequilibrium, especially in the hypersonic case. Hence, predicting the high Mach number shock wave structure will be a challenging test for the accuracy of the kinetic model equations that work well in and near the continuum regime.

In this case the BGK, Shakhov, ES-BGK, and $\nu(c)$-BGK models are used in the UGKS for predicting the shock structure. Their results are compared with the DSMC result [28], which is accepted as a benchmark solution of the Boltzmann equation. This comparison aims at finding the reasons for the advantages and disadvantages of existing kinetic model equations. First, the physical properties predicted by these model equations are compared with DSMC, in order to show the advantages and disadvantages of the modification made by these model equations. Then the model collision terms are qualitatively compared with the Boltzmann collision term using a distribution function in the shock to show the reasons for their advantages and disadvantages.

The upstream and downstream conditions are determined by the Rankine-Hugoniot relation. The density and

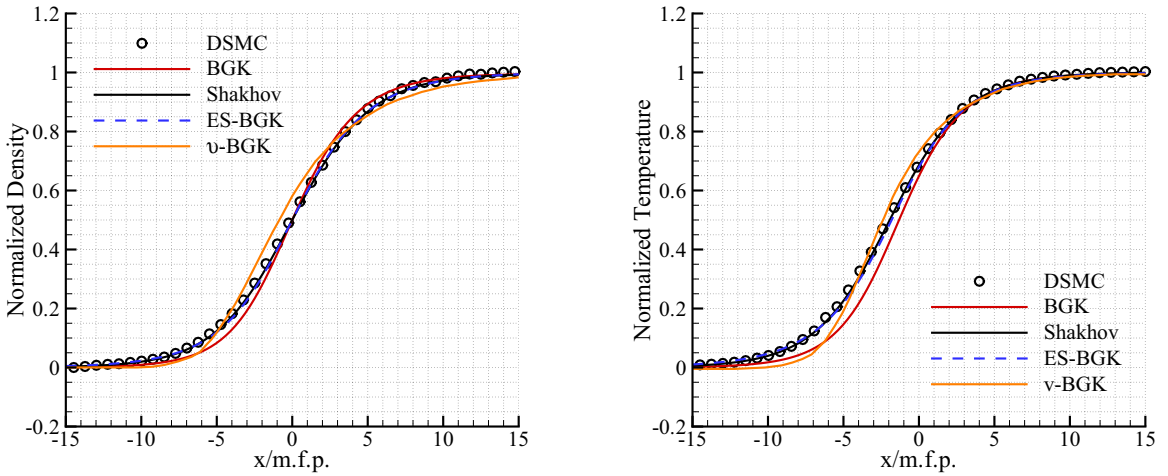

(a) ***Density profile*** (b) ***Temperature profile***

FIG. 2. (Color online) Profile of shock structure with Mach = 1.4.

temperature are normalized by

$$\hat{\rho} = \frac{\rho - \rho_{\text{up}}}{\rho_{\text{down}} - \rho_{\text{up}}}, \quad \hat{T} = \frac{T - T_{\text{up}}}{T_{\text{down}} - T_{\text{up}}}. \tag{22}$$

In this case, both the UGKS and the DSMC solutions use a variable soft sphere (VSS) model, whose the mean free path can be written in terms of ν_{BGK}:

$$l_{mfp} = \frac{4\alpha(5-2\omega)(7-2\omega)}{5(\alpha+1)(\alpha+2)}\sqrt{\frac{kT}{2\pi m}}\frac{1}{\nu_{\text{BGK}}}, \tag{23}$$

where α and ω are scattering parameter and heat index, respectively. For argon gas, $\alpha = 1.40$ and $\omega = 1.78$.

Figures 2 and 3 illustrate the density and temperature profiles in the Mach 1.4 and 8 shock waves, respectively. In the case of a Mach 1.4 shock wave, the density and temperature profiles predicted by the BGK, Shakhov, ES-BGK, and $\nu(c)$-BGK equations match well the benchmark DSMC.

In the case of a Mach 8 shock wave, the results predicted by the kinetic model equations become different from each other and deviate from the benchmark solution. Fig. 3(a) illustrates the density profile in the Mach 8 shock wave structure. The density profile predicted by the Shakhov model matches well that predicted by DSMC, while the ES-BGK and BGK results are steeper and the $\nu(c)$-BGK result displays a kink. Fig. 3(b) illustrates the temperature profiles in the Mach 8 shock wave. Compared with the density profile in Fig. 3(a), the temperature profiles predicted by kinetic model equations deviate much more from the benchmark solution. The result of the Shakhov model deviates from DSMC at the front of the shock, while, in other areas, it matches well the DSMC results. The Shakhov model predicts an overshoot at about $x = 0$, which is phenomenally the same with the DSMC. The $\nu(c)$-BGK predicts a kink again in the temperature profile. Though the results of ES-BGK and BGK are smooth, they deviate from the DSMC results.

The particle distribution functions in $\xi_{\parallel}$ direction of the Mach 1.4 and Mach 8 shock waves are illustrated in Fig. 4, where the distribution functions at different locations in the $x_{\parallel}$ direction are presented. In the case of Mach 1.4, the differences between physical properties before and after the shock are small see Fig. 4(a). Due to these small differences, the distance

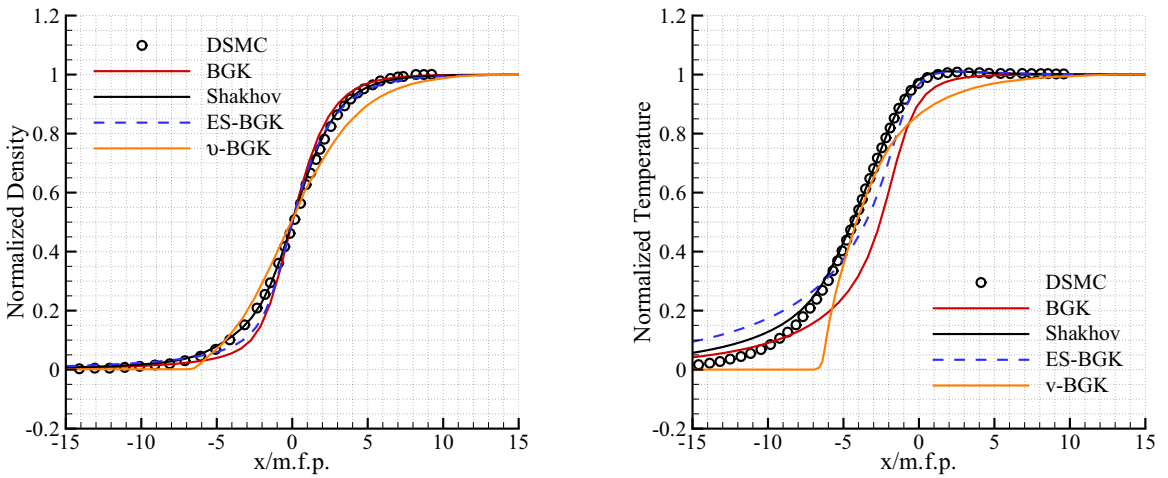

(a) ***Density profile*** (b) ***Temperature profile***

FIG. 3. (Color online) Profile of shock structure with Mach = 8.

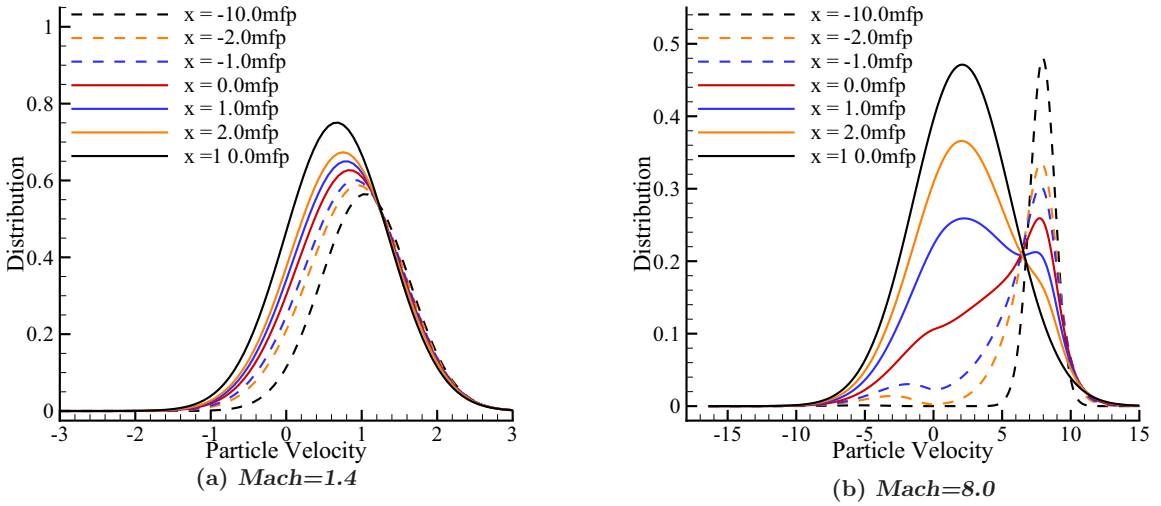

FIG. 4. (Color online) Distribution functions in the shock.

in the velocity space between two clusters of molecules is small (less than $\sqrt{\gamma RT}$, where $\gamma = 5/3$ is the ratio of specific heat for monatomic gas) compared with $\sqrt{3RT_{\rm up}}$, which is the radius of the effect area of upstream distribution. Hence, the distribution in the Mach 1.4 shock wave is nearly monocentric and can even be expressed in a second order Chapman-Enskog expansion. As the Mach number increases, such as in the Mach 8 case illustrated in Fig. 4(b), the distance between two distribution centers in velocity space becomes $7\sqrt{\gamma RT_{\rm up}}$, which is greatly larger than $\sqrt{3RT_{\rm in}}$. Hence the distribution function is bimodal and cannot be approximated by the Chapman-Enskog expansion.

The features of kinetic model equations are analyzed in the rest of this subsection in order to illustrate their difference and their degrees of approximation to the Boltzmann equation. There are two aspects of the nonequilibrium effects: the first aspect comes from the nonequilibrium distribution, and the second comes from the collision term. To determine the nonequilibrium distribution precisely, many methods have been proposed [1,7,26,31,47–49]. When the distribution function is far from equilibrium, such as the distribution in Fig. 4(b), it is difficult to be described by expansion methods [1,47], and the discrete ordinate method (DOM) or discrete velocity method (DVM) should be used, such as in the direct solution of the Boltzmann equiation [31,49] and in the UGKS [7–9,11,42]. Since the kinetic model equations are solved numerically using UGKS, the nonequilibrium distribution function is described precisely, and the deviations of the obtained results are caused mainly by the second aspect associated with the deviations of collision terms.

At the front of the Mach 8 shock wave in Fig. 3, the density is almost the same with the upstream density. Since the mass flux is constant, the velocity at the front of the shock wave is almost the same with the upstream velocity too. In this position, high-speed molecules mix with a small number of low-speed molecules; see the line $x = -2.0$ m.f.p. in Fig. 4(b). The temperature at the front of the shock is much higher than the upstream one.

For the Shakhov collision term in Eq. (11), there is a critical sphere in physical space defined as $|\boldsymbol{c}| = \sqrt{5RT}$ which divides the velocity space into two subspaces. The properties of the Shakhov model in these subspaces and on the critical sphere are shown in Table I.

To analyze the modification made by Shakhov, the collision terms of the Boltzmann equation at the front of the shock are investigated qualitatively and are compared with that of the model collision terms. Before mixing with the low-speed molecules, the distribution of the high-speed molecules is Maxwellian, and it is symmetrical about the face $\xi = u_\parallel$ in velocity space, here $u_\parallel = u_{\rm up}$. After mixing with a small amount of low-speed molecules, the averaged velocity $u_\parallel$ decreases a little. Since the averaged velocity is near $u_{\rm up}$, the peculiar velocities of low-speed molecules are high and contribute significantly to the thermal energy. Thus the temperature rises a large amount.

To simplify the analysis, the two clusters of molecules are supposed to be concentrated at $(u_{\rm up},0,0)$ and $(u_{\rm down},0,0)$ in velocity space, without losing the main feature of distribution function. Thus the distribution function is actually represented by a weighted sum of two δ functions.

TABLE I. The property of the Shakhov model.

	$\lvert\boldsymbol{c}\rvert < \sqrt{5RT}$		$\lvert\boldsymbol{c}\rvert = \sqrt{5RT}$		$\lvert\boldsymbol{c}\rvert > \sqrt{5RT}$	
Direction	$\boldsymbol{c}\cdot\boldsymbol{q} < 0$	$\boldsymbol{c}\cdot\boldsymbol{q} > 0$	$\boldsymbol{c}\cdot\boldsymbol{q} < 0$	$\boldsymbol{c}\cdot\boldsymbol{q} > 0$	$\boldsymbol{c}\cdot\boldsymbol{q} < 0$	$\boldsymbol{c}\cdot\boldsymbol{q} > 0$
Peculiar energy	Low	Low	Critical	Critical	High	High
Sign of $g_{\rm Shakhov} - g_{\rm maxwell}$	+	−	0	0	−	+
Possibility of negative distribution	No	Yes	No	No	Yes	No

The geometrical integration of Boltzmann collision term of the VHS model can be written as

$$\int_{S^2} B(v,\mathbf{\Omega})d\mathbf{\Omega} = -\frac{{d_{\rm ref}}^2 {v_{\rm ref}}^{2\omega-1}}{4}\int_0^{2\pi}\int_0^{\pi} v^{2-2\omega}\sin\chi\, d\chi\, d\varepsilon, \quad (24)$$

where ω is the heat index of molecules, $d_{\rm ref}$ is the reference molecular diameter, and $v_{\rm ref}$ is the reference relative speed. After the collision of $\boldsymbol{\xi} = (u_{\rm down},0,0)$ and $\boldsymbol{\xi_1} = (u_{\rm up},0,0)$, ${\xi'}_{\parallel}$, the component of the postcollision velocity in the axial direction is in the form of

$${\xi'}_{\parallel} = \frac{2\cos\chi}{v} + \frac{u_{\rm up}+u_{\rm down}}{2}. \quad (25)$$

Thus the geometrical integration can be written in terms of ${\xi'}_{\parallel}$ as

$$\frac{{d_{\rm ref}}^2 {v_{\rm ref}}^{2\omega-1}}{2}\int_0^{2\pi}\int_{-v/2}^{v/2} v^{1-2\omega}\, d{\xi'}_{\parallel}\, d\varepsilon. \quad (26)$$

Since $v = u_{\rm up} - u_{\rm down}$ is a constant in the collision of $\boldsymbol{\xi} = (u_{\rm down},0,0)$ and $\boldsymbol{\xi_1} = (u_{\rm up},0,0)$ molecules, postcollision molecules with different ${\xi'}_{\parallel}$ are uniformly distributed in a closed interval $[u_{\rm down},u_{\rm up}]$.

The distribution of postcollision molecules predicted by the BGK model and the Shakhov model are

$$\begin{aligned} g_{\parallel\rm BGK} &= n\left(\frac{m}{2\pi kT}\right)^{1/2}\exp\left(-\frac{m{c_{\parallel}}^2}{2kT}\right),\\ g_{\parallel\rm Shakhov} &= g_{\parallel\rm BGK}\left[1+\frac{1-\Pr}{5}\frac{mq_{\parallel}c_{\parallel}}{kTP}\left(\frac{m{c_{\parallel}}^2}{kT}-3\right)\right]. \end{aligned} \quad (27)$$

The $g_{\parallel\rm BGK}$ is a Maxwellian distribution centered at $u_{\parallel}$ with a narrow effective area ($\sqrt{3RT}$). This distribution is obviously far from the uniform distribution. By multiplying $g_{\parallel\rm BGK}$ by a polynomial, the Shakhov model can adjust the distribution of postcollision molecules. Since $\{\xi_{\parallel}|c_{\parallel}<0\}$ covers most part of the interval $[u_{\rm down},u_{\rm up}]$, the distribution of postcollision molecules in $\{\xi_{\parallel}|c_{\parallel}<0\}$ should be investigated. When $c_{\parallel} > -\sqrt{3RT}$, the Shakhov modification depresses the overestimated Maxwellian distribution. When $c_{\parallel} < -\sqrt{3RT}$, the Shakhov modification increases the Maxwellian distribution, which is far less than the uniform distribution. Although this adjustment is rough, it achieves success in this test.

In the ES-BGK model, the temperature is expressed as a tensor. Given $\Pr = 2/3$, the ES-BGK temperature tensor can be expressed as

$$T^{\rm es}_{ij} = \tfrac{3}{2}T\delta_{ij} - \tfrac{1}{2}T_{ij}. \quad (28)$$

The distribution function in the shock wave is axisymmetric, hence $T_{ij} = 0$ when $i \neq j$. The ES-BGK equilibrium distribution can be written as

$$\begin{aligned} g_{\rm es} &= n\left(\frac{m}{2\pi kT^{\rm es}_{\parallel}}\right)^{1/2}\exp\left(-\frac{m}{2kT^{\rm es}_{\parallel}}|\xi_i-u_i|^2\right)\\ &\times\left(\frac{m}{2\pi kT^{\rm es}_{\perp}}\right)^{1/2}\exp\left(-\frac{m}{2kT^{\rm es}_{\perp}}|\xi_j|^2\right)\left(\frac{m}{2\pi kT^{\rm es}_{\perp}}\right)^{1/2}\\ &\times\exp\left(-\frac{m}{2kT^{\rm es}_{\perp}}|\xi_k|^2\right), \end{aligned} \quad (29)$$

where the distribution function is the product of three Maxwellian distributions defined in every three directions; here $T^{\rm es}_{\parallel} = T + 1/2(T - T_{\parallel})$ is less than $T^{\rm es}_{\perp} = T + 1/2(T - T_{\perp})$, since $T_{\parallel}$ is larger than $T_{\perp}$. This ES-BGK equilibrium functions as a feedback regulation: if inputting a big $T_{\parallel}$, the output relaxation rate is a large in the $\xi_{\parallel}$ direction, which will decrease $T_{\parallel}$ consequently. When the shape of distribution is similar to a ellipsoid, the big $T_{\parallel}$ means that the shape of distribution stretches significantly in the $\xi_{\parallel}$ direction, and the portion of high-speed molecules in this direction is larger than that in the $\xi_{\perp}$ direction with a small temperature $T_{\parallel}$. Since the high-speed molecules collide more often, the high energy associated with the big $T_{\parallel}$ will transport to the other directions quickly and consequently decrease $T_{\parallel}$ to a large degree. So when the shape of distribution is similar to a ellipsoid (Fig.4(a)), the ES-BGK model fits the physical reality well (Fig. 2).

In the $\nu(c)$-BGK model, the relaxation rate is velocity dependent. Though $\nu(c)$-BGK kinks in both density and temperature profiles and deviate significantly from the DSMC results, the model predicts a lower temperature in the front of the shock, which is important for the Shakhov model, BGK, and ES-BGK model whose relaxation rates are independent on velocity. The relation between the molecular velocity and the relaxation rate in the $\nu(c)$-BGK model is defined as a polynomial of molecular velocity. It qualitatively describes the reality that high-speed molecules collide more often, while the qualitative value of the relaxation rate may deviate significantly from the Boltzmann one in certain cases, which will be illustrated in the next subsection. The success of $\nu(c)$-BGK in depressing the temperature at the front of the shock implies that the relaxation rate of high-speed molecules predicted by the other models may be lower than the reality, while the modification of $\nu(c)$-BGK rises it too much.

In this subsection, a shock wave structure case is carried out, where the nonequilibrium is mainly caused by the separated distributions of high- and low-speed molecules. From the above analysis, it can be seen that although these modified models all give a correct Prandtl number, their relaxation processes are largely different from each other. The relaxation process of the Shakhov model fits the Boltzmann relaxation process well by using the information of nonequilibrium heat flux well for indicating the modification of relaxation rates in the velocity space. Although the Shakhov did best among these kinetic models, it should still face a deficiency in that it predicts a early rise at the front of the shock wave in the temperature profile shown in Fig. 3(b). Since the $\nu(c)$-BGK model successfully depresses the temperature at this point, and its velocity-dependent relaxation rate relates to the high-speed molecules closely, the effects of the high-speed and energetic molecules will be carefully examined in the next test case.

B. The homogenous relaxation case

The exact solution of the nonlinear Boltzmann equation for spatially homogeneous problems has been well studied in Refs. [37–39,50]. Their studies are originally motivated by the quantitative calculation of certain gas-phase reactions

and chemical reactions in the case of a highly nonequilibrium initial distribution. These gas-phase and chemical reactions relate mostly to the collision between high-speed molecules, which is also important for highly nonequilibrium gas flows without these reactions.

Since the spacial homogeneous assumption is used in the solution process, $\boldsymbol{\xi} \cdot \nabla_x f$ in the Boltzmann equation is zero. Then the Boltzmann equation is simplified as

$$\frac{\partial f}{\partial t} = I(f,f). \tag{30}$$

The relaxation processes of the Boltzmann equation and kinetic model equations are carefully examined in this case. Since both the initial condition and the relaxation process are spherically symmetrical, the heat flux is zero, and the temperatures are isotropic. Thus both the Shakhov model and the ES-BGK model are reduced to the BGK model. The highly nonequilibrium is mainly due to the non-Maxwellian distribution in the radial direction. In this special case in a purely kinetic regime, the phenomenal difference between the Boltzmann collision term and the BGK collision term is that the relaxation rate of the BGK collision term is a local constant which is independent of velocity and is obviously unphysical. The aim of carrying out this test case is to investigate to what extent the unphysical relaxation rate can affect the accuracy, in order to determine whether it needs to be modified or not in the scope of the numerical prediction.

An isotropic scattering Maxwell model is used in this case, whose collision kernel is defined as

$$B(v,g) = g\sigma(g,\chi), \tag{31}$$

where $\sigma(g,\chi)$ is the differential cross section of this model:

$$\sigma(g,\chi) = \kappa\phi(\chi)/g, \tag{32}$$

and the below equation holds:

$$\int_0^{\pi} \phi(\chi)\sin\chi\, d\chi = 2. \tag{33}$$

Given the expression of $d\boldsymbol{\Omega}$,

$$d\boldsymbol{\Omega} = \sin\chi\, d\chi\, d\varepsilon, \tag{34}$$

where ε is the azimuth angle which varies form 0 to 2π, χ is the scattering angle which varies from 0 to π, the collision term can be written as

$$\begin{aligned} I(\boldsymbol{\xi}) = &\int_{R^3}\int_0^{2\pi}\int_0^{\pi} f(\boldsymbol{\xi}_1')f(\boldsymbol{\xi}')\kappa\phi(\chi)\sin\chi\, d\chi\, d\varepsilon\, d\boldsymbol{\xi}_1 \\ &- \int_{R^3}\int_0^{2\pi}\int_0^{\pi} f(\boldsymbol{\xi}_1)f(\boldsymbol{\xi})\kappa\phi(\chi)\sin\chi\, d\chi\, d\varepsilon\, du_1, \end{aligned} \tag{35}$$

and simplified as

$$I(v) = R - 4\pi n\kappa f(\boldsymbol{\xi}), \tag{36}$$

where $4\pi n\kappa$ is the collision frequency independent of velocity and is constant in the whole velocity space. This collision frequency equals two times of the relaxation rate of BGK model.

In this subsection, it is supposed that the Boltzmann collision term can be split into a BGK collision term and a residual Δ in the following form:

$$I(\boldsymbol{\xi}) = I_{\mathrm{BGK}}(\boldsymbol{\xi}) + \Delta. \tag{37}$$

The following part of this subsection is a detailed comparison of the Boltzmann and the BGK equations.

Normalize the time τ and the peculiar velocity c with reference time $4n\pi\kappa$ and reference velocity $\sqrt{kT}$, respectively; then the analytical solution process can be written as [39]

$$f(c,\tau) = \frac{\exp\left[\frac{-c^2}{2\alpha(\tau)}\right]}{[2\pi\alpha(\tau)]^{3/2}}\left[\frac{5\alpha(\tau)-3}{2\alpha(\tau)} + \frac{1-\alpha(\tau)}{2\alpha(\tau)^2}c^2\right], \tag{38}$$

where $\alpha(\tau) = 1 - \exp(-\tau/6)$, while the analytical solution of relaxation BGK equation has the following form:

$$f(c,\tau) = g(c) + \exp\left(\frac{\tau\nu}{2}\right)[f(c,0) - g(c)]. \tag{39}$$

Given the analytical solution, the value of the Boltzmann operator can also be obtained; it is written as

$$\begin{aligned} &I_{\mathrm{Boltzmann}}(u) \\ &= \frac{15 + 10e^{\tau/6}(-3+c^2) + e^{\tau/3}(15 - 10c^2 + c^4)}{12(-1+e^{\tau/6})^2[5 + 2e^{\tau/3} + e^{\tau/6}(-7+c^2)]} f(c,\tau). \end{aligned} \tag{40}$$

Since the distribution function is symmetrical in this case, the odd order moments are zero, and the even order moment at random time is

$$m(2n,\tau) = \int_{R^3} c^{2n} f(c,\tau)\, dc. \tag{41}$$

For convenience, the moments are normalized by their final equilibrium value when $\tau \to \infty$. Thus the normalized even moments are defined as

$$M(2n,\tau) = m(2n,\tau)/m(2n,\infty). \tag{42}$$

Calculating the even order moments of the solution of Boltzmann equation (38) and BGK equation (39), the analytical time evolution of the normalized moments can be obtained as

$$M(2n,\tau) = \alpha(\tau)^{2n-1}[2n - (2n-1)\alpha(\tau)], \tag{43}$$

and the BGK's moment evolution is

$$M(2n,t) = 1 + e^{-\frac{t}{\tau}}[M(2n,0) - 1]. \tag{44}$$

The initial distribution and the final equilibrium distribution of this case are illustrated in Fig. 5 on a random plane which passes through the origin (0,0,0) in velocity space. The time evolutions of distribution functions, which are obtained using the Boltzmann equation and the BGK model equation, respectively, are illustrated in Fig. 6(a). The BGK solution matches the Boltzmann solution well in whole velocity space, except in a small interval around $v = 0$, where the deviation is obvious when $\tau \in (0,3)$, since the nonequilibrium effect plays a dominant role in such a time interval. Different from the Shakhov and the ES-BGK models, the $\nu(c)$-BGK model cannot be reduced to BGK in this case. The time evolution of distribution functions predicted

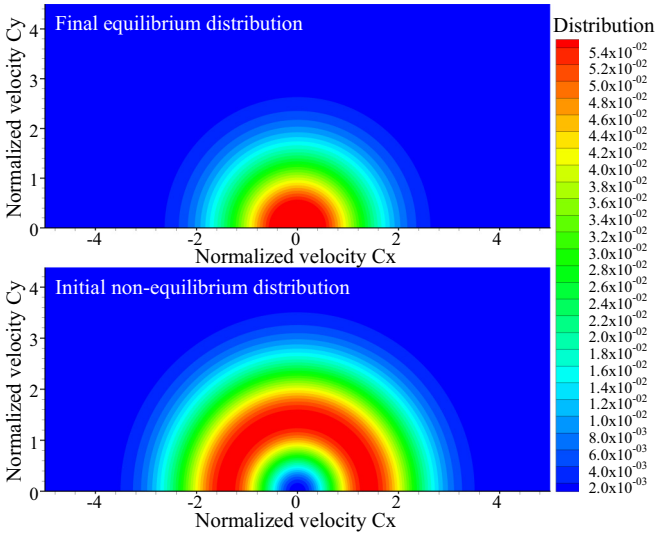

FIG. 5. (Color online) The initial and final distribution of the homogenous relaxation problem.

by the $\nu(c)$-BGK model are shown in Fig. 7. The below velocity-dependent relaxation rates, which were suggested in Ref. [45], are used in this test and are illustrated in Fig. 7(a) to Fig. 7(d):

$$\begin{aligned}
\nu &= \nu_{\mathrm{BGK}}(0.431587c^{1.791288}),\\
\nu &= \nu_{\mathrm{BGK}}[0.0268351(1+14.2724c^{2})],\\
\nu &= \nu_{\mathrm{BGK}}(0.0365643[1+10c^{2.081754})],\\
\nu &= \nu_{\mathrm{BGK}}(0.1503991[1+0.92897c^{4})].
\end{aligned} \tag{45}$$

Each of these relaxation rates in Eq. (45) can give a correct Prandtl number, while their relaxation processes are largely different and deviate significantly from both the Boltzmann process and BGK process. In the rest of this subsection, this paper focuses on examining the Boltzmann process and the BGK process.

Though the evolution of distribution predicted by BGK matches the Boltzmann one well in Fig. 6(a), its evolution of high order moments deviates significantly from the Boltzmann one in Fig. 6(b). To find the reason for the large deviation of high order moments predicted by the BGK equation, the values of the Boltzmann operator and BGK operator at different times are compared in Fig. 8. From Fig. 8(a) it can be seen that before three mean collision times, the deviations are mainly in the central interval around $c = 0$, and the two operators start to match well with each other after three mean collision times when the shape of distribution function approaches equilibrium and the nonequilibrium effect becomes weak. However, the information illustrated in Fig. 8(a) is not sufficient for finding the reason for the large deviation of high order moments. To better illustrate the difference between the two operators, Fig. 8(b) illustrates the value of $rate(c) = I_{\mathrm{BGK}}(c)/I_{\mathrm{Boltzmann}}(c)$ at different times. The presence of large values of $rate(c)$ at about $c = 1$ and $c = 2$ in Fig. 8(b) is due to the BGK and Boltzmann operators having different zero points, which are illustrated in Fig. 8(a). The ratio approaches unity in the whole velocity space as the distribution function approaches Maxwellian. At the time $t = 0$, in $c \in (0,2)$, whether positive or negative, the absolute value of the BGK collision term is less than the Boltzmann one, and the ratio is near 0.8; in $c \in (2,\infty)$ for high-speed molecules, the collision terms are positive, and as c increases, the ratio increases quickly. One may think that the deviation and the fast convergence of the high order moments illustrated in Fig. 6(b) may occur because of the large value of $rate(c)$ for high-speed molecules in Fig. 8(b). Let us multiply Δ, the difference of the BGK and Boltzmann operators, by 1 and c^8; the results are plotted in Fig. 9. The difference of operators are enormous in $c \in (0,1)$, as illustrated in Fig. 9(a), but, when multiplied by c^8, the values become small, as illustrated in Fig. 9(b). For high-speed molecules located in $c \in (3,\infty)$, due to their values of the distribution function being small, the difference between the two operators is also small and can be ignored which is shown in Fig. 9(a), but when multiplied by high order c^n, they contribute significantly and become

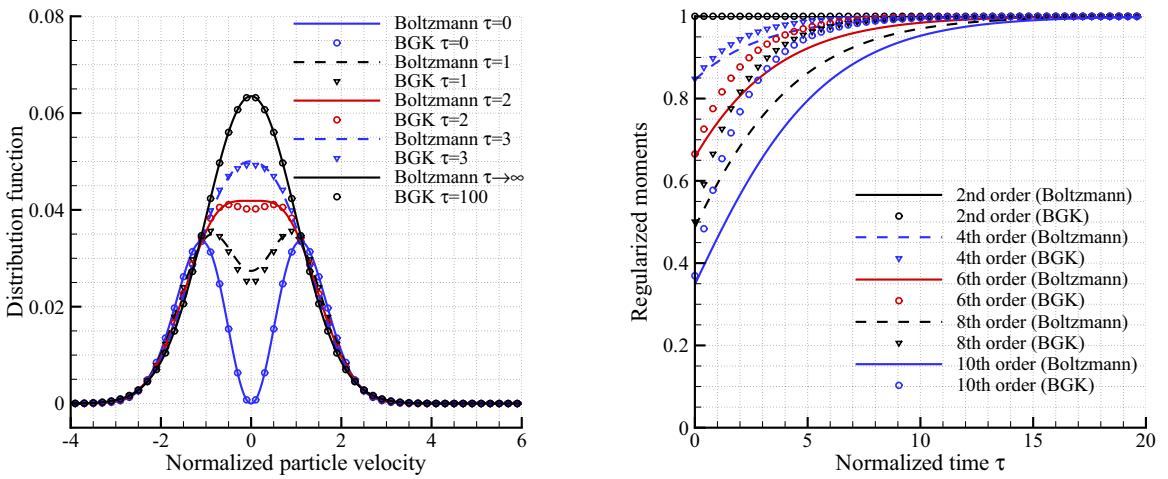

(a) *Time evolution of distribution function* (b) *Time evolution of moments*

FIG. 6. (Color online) Time evolution of distribution function and moment of BGK solution and BKW solution.

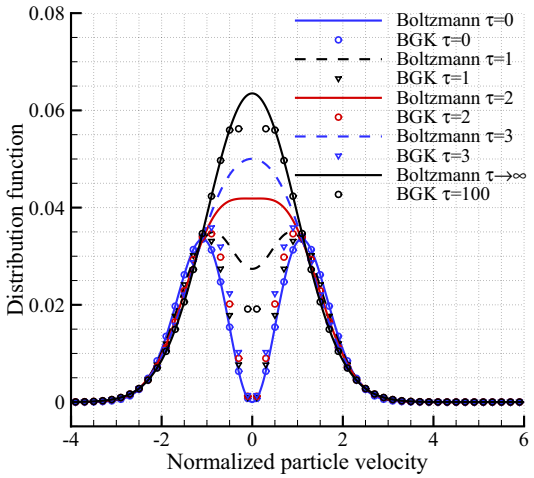

(a) $\nu = \nu_{BGK}\left(0.431587c^{1.791288}\right)$

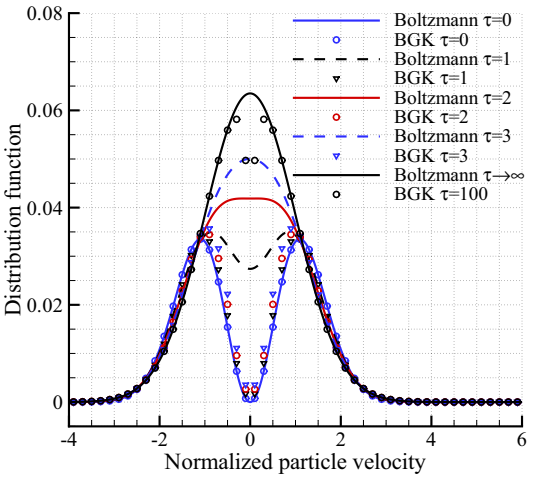

(b) $\nu = \nu_{BGK}\left(0.0268351\left(1 + 14.2724c^2\right)\right)$

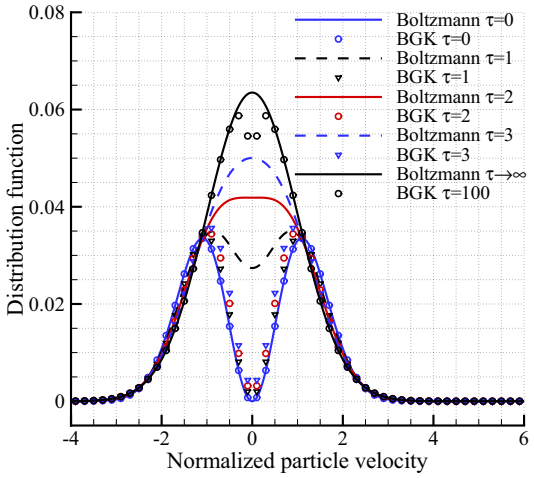

(c) $\nu = \nu_{BGK}\left(0.0365643\left(1 + 10c^{2.081754}\right)\right)$

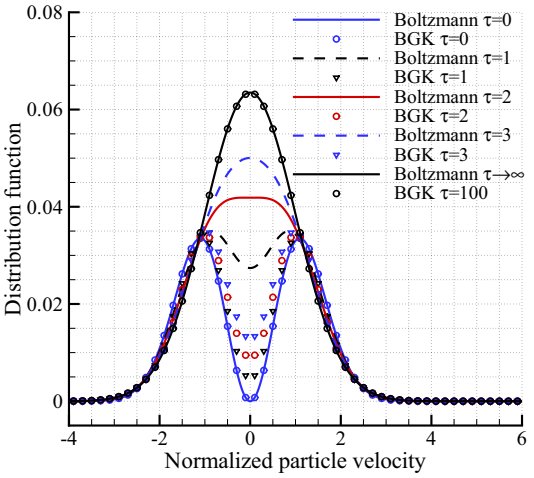

(d) $\nu = \nu_{BGK}\left(0.1503991\left(1 + 0.92897c^4\right)\right)$

FIG. 7. (Color online) Time evolution of distribution function predicted using different ν-BGK models.

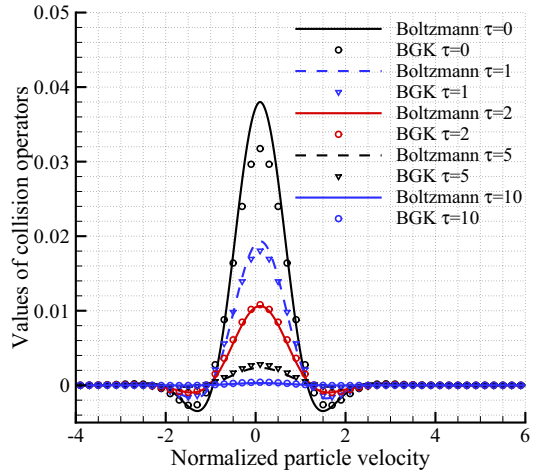

(a) ***the values of collision terms***

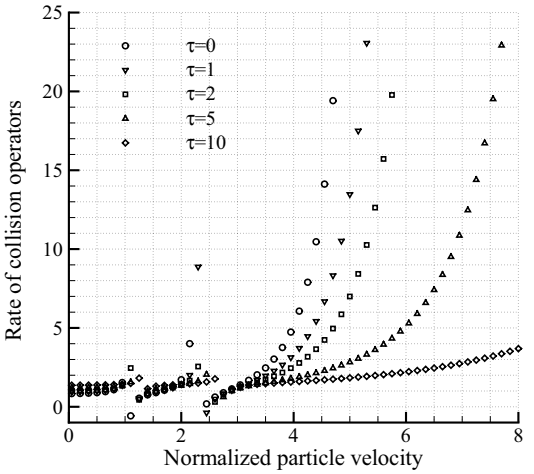

(b) ***the rate of BGK to Boltzmann***

FIG. 8. (Color online) Collision terms of BGK and Boltzmann and their rate.

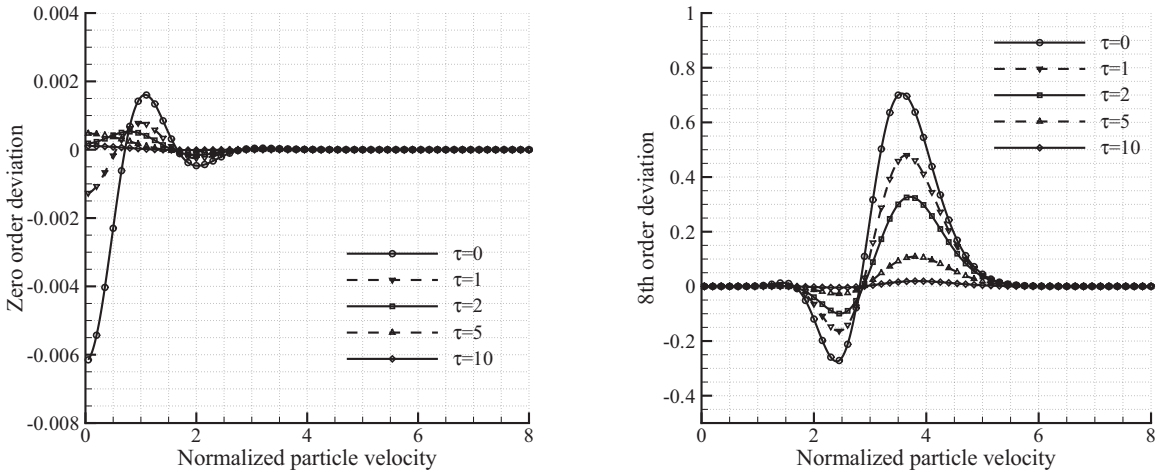

(a) *Zero order moment* (b) *Eighth or dermoment*

FIG. 9. Moment deviation in velocity space.

more and more important when n becomes larger, such as in Fig. 9(b).

From the above analysis, it can be seen that though the value of the BGK operator matches well that of the Boltzmann operator in Fig. 6(a), due to its velocity-independent relaxation rate, the relaxation rate of high-speed molecules are overestimated in the BGK model. As n becomes large, the overestimated relaxation rate becomes important and leads to an overestimated high relaxation rate of moments illustrated in Fig. 6(b). The BGK, the ES-BGK, and the Shakhov equations ignore the velocity-dependent relaxation rate, while the $\nu(c)$-BGK equation adopts an unphysical one. To predict this case precisely using kinetic models, the velocity-dependent relaxation rate should be taken into consideration carefully in later kinetic models.

V. THE RELATIONSHIP BETWEEN THE BOLTZMANN EQUATION AND BGK EQUATION

In Sec. IV the difference between the kinetic model equations and the Boltzmann equation were investigated. We conclude that the asymmetrical distribution and the velocity-dependent collision frequency are the reasons for the deviations in two cases. To reveal the difference explicitly and quantitatively, a relationship between the BGK equation and the Boltzmann equation should be derived. To derive such a relationship, the distribution function f is decomposed into an equilibrium distribution g and a deviation h from the equilibrium state. Submit $f = g + h$ into Eq. (2), and it becomes

$$\begin{aligned} I(\boldsymbol{\xi}) = &\int_{R^3}\int_{S^2} [g(\boldsymbol{\xi}_1')g(\boldsymbol{\xi}') - g(\boldsymbol{\xi}_1)g(\boldsymbol{\xi})]B(v,\boldsymbol{\Omega})d\boldsymbol{\Omega}\, d\boldsymbol{\xi}_1 \\ &+ \int_{R^3}\int_{S^2} [h(\boldsymbol{\xi}_1')h(\boldsymbol{\xi}') - h(\boldsymbol{\xi}_1)h(\boldsymbol{\xi})]B(v,\boldsymbol{\Omega})d\boldsymbol{\Omega}\, d\boldsymbol{\xi}_1 \\ &+ \int_{R^3}\int_{S^2} [g(\boldsymbol{\xi}_1')h(\boldsymbol{\xi}') - g(\boldsymbol{\xi}_1)h(\boldsymbol{\xi})]B(v,\boldsymbol{\Omega})d\boldsymbol{\Omega}\, d\boldsymbol{\xi}_1 \\ &+ \int_{R^3}\int_{S^2} [h(\boldsymbol{\xi}_1')g(\boldsymbol{\xi}') - h(\boldsymbol{\xi}_1)g(\boldsymbol{\xi})]B(v,\boldsymbol{\Omega})d\boldsymbol{\Omega}\, d\boldsymbol{\xi}_1. \end{aligned} \tag{46}$$

With more detailed information of particle collisions, Eq. (46) can be simplified. The postcollision velocities can be specified by the precollision ones and the solid angle $\boldsymbol{\Omega}$ in the form

$$\begin{aligned} \boldsymbol{\xi}' &= \frac{\boldsymbol{\xi}_1 + \boldsymbol{\xi}}{2} + \frac{|\boldsymbol{\xi}_1 - \boldsymbol{\xi}|}{2}\boldsymbol{\Omega}, \\ \boldsymbol{\xi}_1' &= \frac{\boldsymbol{\xi}_1 + \boldsymbol{\xi}}{2} - \frac{|\boldsymbol{\xi}_1 - \boldsymbol{\xi}|}{2}\boldsymbol{\Omega}. \end{aligned} \tag{47}$$

The expression of the isotropic scattering collision kernel is $C_d v^{(d-5)/(d-1)}$. When $d \to \infty$, it represents the hard sphere model. When d is finite, it represents the widely used variable hard sphere model, where d relies on the heat index of real molecules.

The third term on the RHS of Eq. (46) can be written as

$$\begin{aligned} &\int_{R^3}\int_{S^2} g(\boldsymbol{\xi}_1')h(\boldsymbol{\xi}')B(v,\boldsymbol{\Omega})d\boldsymbol{\Omega}\, d\boldsymbol{\xi}_1 \\ &= \int_{R^3}\int_0^{2\pi}\int_0^{\pi} g\left(\frac{\boldsymbol{\xi}_1 + \boldsymbol{\xi}}{2} - \frac{|\boldsymbol{\xi}_1 - \boldsymbol{\xi}|}{2}\boldsymbol{\Omega}\right) h\left(\frac{\boldsymbol{\xi}_1 + \boldsymbol{\xi}}{2} + \frac{|\boldsymbol{\xi}_1 - \boldsymbol{\xi}|}{2}\boldsymbol{\Omega}\right) C_d v^{(d-5)/(d-1)} \sin(\chi) d\chi\, d\varepsilon\, d\boldsymbol{\xi}_1. \end{aligned} \tag{48}$$

Replace $\boldsymbol{\Omega}$ by $-\boldsymbol{\Omega}_1$, so χ is replaced by $\pi - \chi_1$, and ε is replaced by $\pi + \varepsilon_1$; the integral can be further written as

$$\int_{R^3}\int_{\pi}^{3\pi}\int_0^{\pi} g\left(\frac{\boldsymbol{\xi}_1 + \boldsymbol{\xi}}{2} + \frac{|\boldsymbol{\xi}_1 - \boldsymbol{\xi}|}{2}\boldsymbol{\Omega}_1\right) h\left(\frac{\boldsymbol{\xi}_1 + \boldsymbol{\xi}}{2} - \frac{|\boldsymbol{\xi}_1 - \boldsymbol{\xi}|}{2}\boldsymbol{\Omega}_1\right) C_d v^{(d-5)/(d-1)} \sin(\chi_1) d\chi_1\, d\varepsilon_1\, d\boldsymbol{\xi}_1. \tag{49}$$

The starting angle of ε can be randomly chosen. After removing the "1" subscript of $\mathbf{\Omega}_1$, χ_1, and ε_1, the integral is finally written as

$$\int_{R^3}\int_0^{2\pi}\int_0^{\pi} g\left(\frac{\boldsymbol{\xi}_1+\boldsymbol{\xi}}{2}-\frac{|\boldsymbol{\xi}_1-\boldsymbol{\xi}|}{2}\mathbf{\Omega}\right) h\left(\frac{\boldsymbol{\xi}_1+\boldsymbol{\xi}}{2}+\frac{|\boldsymbol{\xi}_1-\boldsymbol{\xi}|}{2}\mathbf{\Omega}\right) C_d v^{(d-5)/(d-1)}\sin(\chi)d\chi\, d\varepsilon\, d\boldsymbol{\xi}_1$$
$$=\int_{R^3}\int_{S^2} h(\boldsymbol{\xi}_1')g(\boldsymbol{\xi}')B(v,\mathbf{\Omega})d\mathbf{\Omega}\, d\boldsymbol{\xi}_1. \tag{50}$$

Thus the following equation can be obtained:

$$\int_{R^3}\int_{S^2} g(\boldsymbol{\xi}_1')h(\boldsymbol{\xi}')B(v,\mathbf{\Omega})d\mathbf{\Omega}\, d\boldsymbol{\xi}_1 = \int_{R^3}\int_{S^2} h(\boldsymbol{\xi}_1')g(\boldsymbol{\xi}')B(v,\mathbf{\Omega})d\mathbf{\Omega}\, d\boldsymbol{\xi}_1. \tag{51}$$

The equilibrium states lead to the zero value collision terms, hence

$$\int_{R^3}\int_{S^2}[g(\boldsymbol{\xi}_1')g(\boldsymbol{\xi}')-g(\boldsymbol{\xi}_1)g(\boldsymbol{\xi})]v\sigma(v,\chi)\,d\mathbf{\Omega}\, d\boldsymbol{\xi}_1\equiv 0. \tag{52}$$

Submit Eq. (50) and Eq. (52) into Eq. (46), and it can be further arranged as

$$I(\boldsymbol{\xi})=\int_{R^3}\int_{S^2}[h(\boldsymbol{\xi}_1')+2g(\boldsymbol{\xi}_1')]h(\boldsymbol{\xi}')B(v,\mathbf{\Omega})d\mathbf{\Omega}\, d\boldsymbol{\xi}_1 - \int_{R^3}\int_{S^2}[g(\boldsymbol{\xi})h(\boldsymbol{\xi}_1)+h(\boldsymbol{\xi})f(\boldsymbol{\xi}_1)]B(v,\mathbf{\Omega})d\mathbf{\Omega}\, d\boldsymbol{\xi}_1. \tag{53}$$

The collision frequency, the equilibrium collision frequency, and the deviation collision frequency are defined by the following integrals, respectively:

$$\begin{aligned}\nu &= \int_{R^3}\int_{S^2} f(\boldsymbol{\xi}_1)B(v,\mathbf{\Omega})d\mathbf{\Omega}\, d\boldsymbol{\xi}_1,\\ \nu_{\mathrm{eq}} &= \int_{R^3}\int_{S^2} g(\boldsymbol{\xi}_1)B(v,\mathbf{\Omega})d\mathbf{\Omega}\, d\boldsymbol{\xi}_1,\\ \nu_{\mathrm{dev}} &= \int_{R^3}\int_{S^2} h(\boldsymbol{\xi}_1)B(v,\mathbf{\Omega})d\mathbf{\Omega}\, d\boldsymbol{\xi}_1.\end{aligned} \tag{54}$$

Given Eq. (54), the last term in Eq. (53) can be written in the form

$$\nu(g(\boldsymbol{\xi})-f(\boldsymbol{\xi}))-\nu_{\mathrm{dev}}g(\boldsymbol{\xi}). \tag{55}$$

Thus, the Boltzmann collision term is finally simplified as

$$I(\boldsymbol{\xi})=\nu(g(\boldsymbol{\xi})-f(\boldsymbol{\xi}))-\nu_{\mathrm{dev}}g(\boldsymbol{\xi})+\int_{R^3}\int_{S^2}[2g(\boldsymbol{\xi}_1') + h(\boldsymbol{\xi}_1')]h(\boldsymbol{\xi}')B(v,\mathbf{\Omega})d\mathbf{\Omega}\, d\boldsymbol{\xi}_1. \tag{56}$$

Here the collision term is split into two parts, a BGK relaxation part along with a non-BGK residual which includes $\nu_{\mathrm{dev}}g(\boldsymbol{\xi})$ and an inverse collision-related integral which is temporally named the deviation integral and denoted by I_{dev} in this paper.

Equation (56) is a relationship between the original BGK equation [5] and the Boltzmann equation. Their difference is written as $\nu_{\mathrm{dev}}g(\boldsymbol{\xi})+I_{\mathrm{dev}}$. The BGK part in Eq. (56) describes the impacts of local deviation, while the non-BGK residual describes the impacts of global deviations since the deviations in the rest of the velocity space determine the values of ν_{dev} and I_{dev}.

The BGK collision term used in Eq. (56) is the original one proposed by Bhatnagar, Gross, and Krook in Ref. [5]. When applying a second order Chapman-Enskog expansion to this BGK equation and integrating the resulting equation with respect to $\boldsymbol{\xi}$ over the whole velocity space, Navier-Stokes (N-S) equations can be obtained [6]. However, the viscosity coefficient μ in the obtained N-S equations does not match the one obtained by the Boltzmann equation in Ref. [1]. In order to yield a precise viscosity coefficient, the later BGK models replace the collision frequency ν with a free parameter ν_{BGK}. Using the same expansion and integration, Navier-Stokes equations with a viscosity coefficient p/ν_{BGK} are obtained. So the free parameter ν_{BGK} is set to be p/μ.

There exits a relationship between ν_{BGK} and the average equilibrium collision frequency $\bar{\nu}_{\mathrm{eq}}$ in the form [26]

$$\bar{\nu}_{\mathrm{eq}}=M\nu_{\mathrm{BGK}}=\frac{30}{\alpha(5-2\omega)(7-2\omega)}\frac{p}{\mu}, \tag{57}$$

where the heat index ω are properties of a molecular model which depends on d. Thus M is a molecular model-dependent factor. The average equilibrium collision frequency is

$$\bar{\nu}_{\mathrm{eq}}=\frac{1}{n}\int_{R^3}\int_{R^3}\int_{S^2} g(\boldsymbol{\xi}_1)g(\boldsymbol{\xi})B(v,\mathbf{\Omega})d\mathbf{\Omega}\, d\boldsymbol{\xi}_1\, d\boldsymbol{\xi} = 8\sqrt{\pi}C_d n\left(\frac{4kT}{m}\right)^{\frac{d-5}{2(d-1)}}\Gamma\left(\frac{2d-4}{d-1}\right), \tag{58}$$

where Γ is the gamma function. $\bar{\nu}_{\mathrm{eq}}$ is independent on particle velocity, and it depends only on the macroscopic physical properties n, T and the type of molecular models d.

The equilibrium collision depends on the particle velocity:

$$\begin{aligned}\nu_{\mathrm{eq}} &= \int_{R^3}\int_{S^2} g(\boldsymbol{\xi}_1)B(v,\mathbf{\Omega})d\mathbf{\Omega}\, d\boldsymbol{\xi}_1\\ &= \int_{R^3}\int_0^{2\pi}\int_0^{\pi} g(\boldsymbol{\xi}_1)C_d v^{(d-5)/(d-1)}\sin(\chi)d\chi\, d\varepsilon\, d\boldsymbol{\xi}_1\\ &= 4\pi C_d\int_{R^3} g(\boldsymbol{\xi}_1)v^{(d-5)/(d-1)}\, d\boldsymbol{\xi}_1;\end{aligned} \tag{59}$$

for Maxwell molecules the integral can be directly integrated, and $\nu_{\mathrm{eq}}=\bar{\nu}_{\mathrm{eq}}$, while, for other molecules, it needs extra treatments. Write $\boldsymbol{\xi}$ in terms of peculiar velocity $\boldsymbol{c}$ and mean velocity $\boldsymbol{u}$ as $\boldsymbol{\xi}=\boldsymbol{c}+\boldsymbol{u}$ and use the normalized peculiar velocities $\boldsymbol{C}_1=\boldsymbol{c}_1/\sqrt{2kT/m}$ and $\boldsymbol{C}=\boldsymbol{c}/\sqrt{2kT/m}$; then Eq. (59) becomes

$$\nu_{\mathrm{eq}}=4\pi^{-1/2}C_d n\left(\frac{2kT}{m}\right)^{\frac{(d-5)}{2(d-1)}} \times\int_{R^3} e^{-C_1^2}|\boldsymbol{C}_1-\boldsymbol{C}|^{(d-5)/(d-1)}d\boldsymbol{C}_1. \tag{60}$$

Since the integral in Eq. (60) is spherically symmetrical, the value of this integral depends only on scalar variable $|\boldsymbol{C}|$. Thus the integral can be easily obtained using numerical methods.

Given the relation between $\bar{\nu}_{\rm eq}$ and $\nu_{\rm BGK}$ in Eq. (57), Eq. (55) can be rewritten as

$$\frac{M\nu_{\rm eq}}{\bar{\nu}_{\rm eq}} I_{\rm BGK} - \nu_{\rm dev} f(\boldsymbol{\xi}). \tag{61}$$

Submit Eq. (57) and Eq. (61) into Eq. (56) and denote $(M\nu_{\rm eq}(\boldsymbol{\xi}))/\bar{\nu}_{\rm eq}$ by $F(\boldsymbol{\xi})$; then a relationship between the common form of BGK operator and the Boltzmann operator can be obtained in the form

$$I(\boldsymbol{\xi}) = F(\boldsymbol{\xi}) I_{\rm BGK} - \nu_{\rm dev}(\boldsymbol{\xi}) f(\boldsymbol{\xi}) + I_{\rm dev}(\boldsymbol{\xi}). \tag{62}$$

An investigation of the modification made by kinetic models can be carried out now with the aid of Eq. (62). First, the Boltzmann collision term in the form of Eq. (62) is rewritten in a relaxation form for comparison:

$$I(\boldsymbol{\xi}) = F(\boldsymbol{\xi})\nu_{\rm BGK} \left\{ \left[g(\boldsymbol{\xi}) - \frac{\nu_{\rm dev}(\boldsymbol{\xi})}{F(\boldsymbol{\xi})\nu_{\rm BGK}} f + \frac{1}{F(\boldsymbol{\xi})\nu_{\rm BGK}} I_{\rm dev}(\boldsymbol{\xi}) \right] - f(\boldsymbol{\xi}) \right\}. \tag{63}$$

Expand deviation distribution $h(\boldsymbol{\xi})$ around the equilibrium distribution $g(\boldsymbol{\xi})$ using Hermite expansion, and it can be written as

$$h(\boldsymbol{\xi}) = g(\boldsymbol{\xi}) S(\boldsymbol{\xi}), \tag{64}$$

where $S(\boldsymbol{\xi})$ is a linear combination of Hermite polynomials. Using Eq. (64), $I_{\rm dev}$ is written as

$$\begin{aligned} I_{\rm dev} &= \int_{R^3}\int_{S^2} [2 + S(\boldsymbol{\xi}_1')] S(\boldsymbol{\xi}') g(\boldsymbol{\xi}_1') g(\boldsymbol{\xi}') B(v, \boldsymbol{\Omega}) d\boldsymbol{\Omega}\, d\boldsymbol{\xi}_1 \\ &= g(\boldsymbol{\xi}) \int_{R^3}\int_{S^2} [2 + S(\boldsymbol{\xi}_1')] S(\boldsymbol{\xi}') g(\boldsymbol{\xi}_1) B(v, \boldsymbol{\Omega}) d\boldsymbol{\Omega}\, d\boldsymbol{\xi}_1 \\ &= g(\boldsymbol{\xi}) \nu_{I_{\rm dev}}(\boldsymbol{\xi}). \end{aligned} \tag{65}$$

Thus, the collision integral can be expressed in the following relaxation form, which can also be viewed as a general form of the relaxation terms :

$$\begin{aligned} I(\boldsymbol{\xi}) &= F(\boldsymbol{\xi})\nu_{\rm BGK} \left(g(\boldsymbol{\xi}) \left\{ 1 - \frac{\nu_{\rm dev}(\boldsymbol{\xi})[1 + S(\boldsymbol{\xi})]}{F(\boldsymbol{\xi})\nu_{\rm BGK}} + \frac{\nu_{I_{\rm dev}}(\boldsymbol{\xi})}{F(\boldsymbol{\xi})\nu_{\rm BGK}} \right\} - f(\boldsymbol{\xi}) \right) \\ &= F(\boldsymbol{\xi})\nu_{\rm BGK} \{ g(\boldsymbol{\xi})[1 + A(\boldsymbol{\xi})] - f(\boldsymbol{\xi}) \}. \end{aligned} \tag{66}$$

In this generalized relaxation term, $A(\boldsymbol{\xi})$ represents the modification of equilibrium state, and $F(\boldsymbol{\xi})$ represents the modification of relaxation rate. In the shock structure case, the limited success is achieved by the utilization of the information held by nonequilibrium moments, such as the stress and the heat flux, in approximating $A(\boldsymbol{\xi})$. In the homogenous relaxation case, the importance of a velocity-dependent relaxation rate is illustrated.

Compared with Eq. (66), the BGK collision term retains the impacts of local deviation, while the impacts of global deviations $A(\boldsymbol{\xi})$ and the velocity-dependent collision frequency $F(\boldsymbol{\xi})$ are ignored. The $\nu(c)$-BGK model improves the BGK model with a velocity-dependent collision frequency by multiplying $I_{\rm BGK}$ by a function of $\boldsymbol{\xi}$, while $A(\boldsymbol{\xi})$ is left unimproved. The Shakhov and the ES-BGK models try to introduce the information held by nonequilibrium moments to new equilibrium states. The new equilibrium state in the ES-BGK model is in the form of an anisotropic Gaussian, while an asymmetrical Hermite expansion around a Maxwellian is used for the Shakhov model. Both the new equilibrium states can be written in the form $g[1 + E(\boldsymbol{\xi})]$. For the ES-BGK model, $E(\boldsymbol{\xi})$ can be obtained by using Taylor expansion around Maxwellian equilibrium. For the Shakhov model, $E(\boldsymbol{\xi})$ is expressed in terms of Hermite polynomials. Their modifications can be viewed as using $E(\boldsymbol{\xi})$ to approximate $A(\boldsymbol{\xi})$. The existing modified models can predict the continuum gas flows precisely due to the right Prandtl number, while further modification needs to be made to predict the rarefied gas flows precisely. From Eq. (66), it can be seen that the $\nu_{I_{\rm dev}}(\boldsymbol{\xi})$ term in $A(\boldsymbol{\xi})$ is the main difficulty. Since the other terms such as $F(\boldsymbol{\xi})$ and $\nu_{\rm dev}(\boldsymbol{\xi})$ can be directly obtained, one should focus on modeling the $\nu_{I_{\rm dev}}(\boldsymbol{\xi})$ term to construct a new improved model.

The BGK collision term describes that the particle system has the trend towards its local equilibrium. It can be viewed as another description of the second law of thermodynamics. Since using only the second law of thermodynamics is not adequate for governing the detailed relaxation process, additional information is needed. The information can be obtained from the Boltzmann collision term or the patterns of its behavior. Also, the modification of equilibrium and the relaxation rate should be taken into consideration in the later models.

VI. THE ANALYSIS AND TREATMENT OF THE DEVIATION INTEGRAL

Some important features of the deviation integral $I_{\rm dev}(\boldsymbol{\xi})$ are analyzed in this section. First, the mechanism of the influence of a deviation at certain velocity point on another point's evolution of the distribution function is investigated. Here a weak form of the global deviations' impacts is used for convenience:

$$\begin{aligned} &\int_{R^3} (Df(\boldsymbol{\eta})/Dt)_{\rm deviation} \delta(\boldsymbol{\eta} - \boldsymbol{\xi}) d\boldsymbol{\eta} \\ &= \int_{R^3} I_{\rm dev} \delta(\boldsymbol{\eta} - \boldsymbol{\xi}) d\boldsymbol{\eta} \\ &= \int_{R^3}\int_{S^2} \delta(\boldsymbol{\eta} - \boldsymbol{\xi})[f(\boldsymbol{\eta}_1') + g(\boldsymbol{\eta}_1')] h(\boldsymbol{\eta}') B(v, \boldsymbol{\Omega}) d\boldsymbol{\Omega} d\boldsymbol{\eta}_1\, d\boldsymbol{\eta} \\ &= \int_{R^3}\int_{S^2} \delta(\boldsymbol{\eta}' - \boldsymbol{\xi})[f(\boldsymbol{\eta}_1) + g(\boldsymbol{\eta}_1)] h(\boldsymbol{\eta}) B(v, \boldsymbol{\Omega}) d\boldsymbol{\Omega}\, d\boldsymbol{\eta}_1 d\boldsymbol{\eta}, \end{aligned} \tag{67}$$

where δ is a test function, and it is a δ function here. By changing the integral variables from the postcollision velocities to precollision velocities, Eq. (67) is easier to handle. The distribution functions g and f are definitely nonnegative, while the deviation h can be either negative or nonnegative. So the deviation integral can be of either depletion or replenishment. The deviation distribution with velocity $\boldsymbol{\eta}$ can affect the evolution of distribution at $\boldsymbol{\xi}$ through the collision with certain particles at $\boldsymbol{\eta}_1$. Confined by the

geometry of collision, these $\boldsymbol{\eta}_1$ particles should lie on a plane which passes through velocity $\boldsymbol{\xi}$ and is perpendicular to $\boldsymbol{\xi}-\boldsymbol{\eta}_1$. This plane is temporally called the reception plane. Move $\boldsymbol{\eta}_1$ on the reception plane, along the radial direction centered at point $\boldsymbol{\xi}$, and the radius $r=|\boldsymbol{\eta}_1-\boldsymbol{\xi}|$ varies from 0 to infinity. Define $r_0=|\boldsymbol{\eta}-\boldsymbol{\xi}|$ and the relative velocity $v=\sqrt{r^2+r_0^2}$. Since $\sin(\chi)=2\sin(\chi/2)\cos(\chi/2)=\frac{2r_0r}{r^2+r_0^2}$, then $B(v,\boldsymbol{\Omega})d\boldsymbol{\Omega}$ can be written in terms of r and r_0:

$$B(v,\boldsymbol{\Omega})d\boldsymbol{\Omega}=\left(r^2+r_0^2\right)^{\frac{d+3}{2-2d}}2r_0r\,d\chi\,d\varepsilon=p\,d\chi\,d\varepsilon, \quad (68)$$

where the factor p is a weight which has limitations:

$$\lim_{r\to0}p=0,\quad \lim_{r\to\infty}p=\begin{cases}0, d>1,\\ 2r_0, d\to\infty.\end{cases} \quad (69)$$

For finite $d\geqslant 5$, p has a maximum value at $r_{\max}=r_0\sqrt{d-1}/2$, which is some r_0. Since the value of p is different on the reception plane, this deviation impact is determined by the scattering of $f+g$ on the reception plane. Let the moving r be fixed and let r_0 move along the line of $\boldsymbol{\xi}-\boldsymbol{\eta}_1$. Assume the distribution of $f+g$ is concentrated at (r,ε), and the impact is maximum at $r\sqrt{d-1}/2$. It decreases slowly with increasing r_0, while it decreases quickly with decreasing r_0. When r_0 moves into a small interval around 0, the impact of $h(\boldsymbol{\eta})$ is small and is not so important.

Before modeling the deviation integral, a linear integral can first be split from it and leaves a quadratic nonlinear one:

$$\begin{aligned}I_{\text{linear}}+I_{\text{nonlinear}}=&\int_{R^3}\int_{S^2}2g(\boldsymbol{\xi}_1')h(\boldsymbol{\xi}')B(v,\boldsymbol{\Omega})d\boldsymbol{\Omega}\,d\boldsymbol{\xi}_1d\boldsymbol{\xi}\\&+\int_{R^3}\int_{S^2}h(\boldsymbol{\xi}_1')h(\boldsymbol{\xi}')B(v,\boldsymbol{\Omega})d\boldsymbol{\Omega}\,d\boldsymbol{\xi}_1\,d\boldsymbol{\xi}.\end{aligned} \quad (70)$$

The linear term I_{linear} describes the impact of h through the equilibrium state g, while, in a nonlinear term $I_{\text{nonlinear}}$, the impact is through the deviation itself. Confined by the non-negativity of the distribution function, h is in the interval $(-g,+\infty)$ and confined by the integral

$$\int_{R^3}\boldsymbol{\psi}h(\boldsymbol{\xi})\,d\boldsymbol{\xi}\equiv0, \quad (71)$$

where $\boldsymbol{\psi}=(1,\boldsymbol{\xi},|\boldsymbol{\xi}|^2)$. Thus $I_{\text{nonlinear}}$ plays an important role when the deviation is large, while it can be neglected when the distribution function is near equilibrium and the deviation is small. The effect of I_{linear} is always stable no matter the change of the degree of nonequilibrium.

Here we propose a method for modeling the deviation integral I_{dev}. Due to the linearity of I_{linear} with respect to h, one can describe h as series and investigate the impact of each element in this series separately. For example, h can be expanded using the multidimensional Hermite expansion, which is first introduced by Grad for deriving 13 moment equations [47]. The deviation h can also be described by an infinite series of δ functions. When this infinite series is truncated into finite, it is substantially a velocity space discretization and is the same as treating f in the DOM [31,33,34]. For the $I_{\text{nonlinear}}$ term, the Hermite expansion can simplify the form only in terms of moments rather the distribution function, and the DOM will be not efficient for cases with large Mach number and large temperature difference. Inspired by the work of calculating the shock thickness by Mott-Smith [51], where the distribution function in the shock is assumed to be a weighted sum of the Maxwellian distribution from before and after the shock, a method for modeling the I_{dev} term is proposed in this paper. First the distribution function is constructed by using a series of Maxwellian functions. More precisely, the distribution function is described in a function space whose basis functions are the Maxwellian distributions with different locations, heights, and widths. Each Maxwellian distribution represents a cluster of molecules with its own mean velocity and temperature. Due to the flexibility of these Maxwellian functions, the feature of deviation distribution can be captured efficiently, especially for the cases where the distance (in velocity space) between molecule clusters is large, which often occurs in case of high Mach number, and for the cases where the temperature difference is so large that the shape of distribution function of low temperature cluster is almost a spike. Then a standard pattern with only two free parameters will be derived, using which the I_{linear} and $I_{\text{nonlinear}}$ can be reconstructed.

Submit the reconstructed deviation distribution,

$$h=\sum_{n=1}^{\infty}A_\alpha g(\boldsymbol{u},T_\alpha), \quad (72)$$

where A_α is the weight, into I_{linear}, and normalize $\boldsymbol{\xi}$ as $\boldsymbol{C}=(\boldsymbol{\xi}-\boldsymbol{u})/\sqrt{kT/m}$, and v as $V=v/\sqrt{kT/m}$; after rearrangements, I_{linear} becomes

$$n\left(\frac{kT}{m}\right)^{\frac{1+d}{1-d}}\sum_{\alpha=0}^{\infty}A_\alpha D_\alpha(\boldsymbol{C}), \quad (73)$$

where

$$D_\alpha(\boldsymbol{C})=\int_{S^2}G(\boldsymbol{C}'_1)G_\alpha(\boldsymbol{C}')B(V,\boldsymbol{\Omega})d\Omega\,d\boldsymbol{C}_1. \quad (74)$$

Here G is a standard multidimensional normal distribution, and G_α is a also a normal distribution in the form

$$G_\alpha(\boldsymbol{C}')=\left(\frac{1}{2\pi\hat{T}}\right)^{3/2}\exp\left(-\frac{1}{2\hat{T}}|\boldsymbol{C}'-\hat{\boldsymbol{U}}|^2\right), \quad (75)$$

where $\hat{T}=T_\alpha/T$, $\hat{\boldsymbol{U}}=(\boldsymbol{u}_\alpha-\boldsymbol{u})/\sqrt{kT/m}$. Using Eq. (73), the I_{liner} can be reconstructed with $D_n(\boldsymbol{C})$.

Using the same methodology, submit Eq. (72) into $I_{\text{nonlinear}}$; consequently $I_{\text{nonlinear}}$ can be reconstructed as

$$n\sum_{\beta=0}^{\infty}A_\beta\left(\frac{kT_\beta}{m}\right)^{\frac{1+d}{1-d}}\sum_{\alpha=0}^{\infty}A_\alpha D_{\beta\alpha}(\boldsymbol{C}), \quad (76)$$

where

$$D_{\beta\alpha}(\boldsymbol{C})=\int_{S^2}G(\boldsymbol{C}'_1)G_{\beta\alpha}(\boldsymbol{C}')B(V,\boldsymbol{\Omega})d\Omega\,d\boldsymbol{C}_1. \quad (77)$$

Here $G_{\beta\alpha}$ has the same form with G_α in Eq. (75) except that $\hat{T}=T_\alpha/T_\beta,\hat{\boldsymbol{U}}=(\boldsymbol{u}_\alpha-\boldsymbol{u}_\beta)/\sqrt{kT_\beta/m}$. Compare $D_{\beta\alpha}$ and D_α, and it can be seen that D_α is a special case of $D_{\beta\alpha}$ when the β state is the local equilibrium state. Thus using $D_{\beta\alpha}$, both I_{linear} and $I_{nonliner}$ can be reconstructed.

In $D_{\beta\alpha}(\boldsymbol{C})$, G and $G_{\beta\alpha}$ are two normal distribution functions, and G is in a standard form. Physically speaking G and

$G_{\beta\alpha}$ represent two clusters of normal distributed molecules, and $D_{\beta\alpha}(\boldsymbol{C})$ describes the replenishment to the molecules with peculiar velocity $\boldsymbol{C}$ through the binary collisions of these two molecule clusters. So $D_{\beta\alpha}(\boldsymbol{C})$ can be viewed as a standard replenishment term and can be used as a pattern for the reconstruction of the deviation integral $I_{\rm dev}$. Since G is a standard normal distribution, $D_{\beta\alpha}(\boldsymbol{C})$ depends only on the temperature ratio $\hat{T}$ and the velocity difference $\hat{\boldsymbol{U}}$. Moreover, $D_{\beta\alpha}(\boldsymbol{C})$ has spherical symmetry, and thus the dependence on $\hat{\boldsymbol{U}}$ is reduced to a dependence on $|\hat{\boldsymbol{U}}|$. So the pattern $D_{\beta\alpha}(\boldsymbol{C})$ has only two free parameters. When the α and β states are given, the two parameters of $D_{\beta\alpha}(\boldsymbol{C})$ are directly obtained, and the replenishment to the molecules with velocity $\boldsymbol{\xi} = \sqrt{kT_\beta/m}\boldsymbol{C} + \boldsymbol{u}_\beta$ can be obtained by multiplying the $D_{\beta\alpha}(\boldsymbol{C})$ pattern with $nA_\beta A_\alpha (kT_\beta/m)^{(1+d)/(1-d)}$, which is shown in Eq. (76). Sum the replenishment terms of all related α and β states, and $I_{\rm dev}$ can be obtained. Thus $I_{\rm dev}$ is modeled by the reconstruction of D patterns. The investigation of the properties of D patterns with varying parameters could be helpful to understand the physics of deviation of integrals, and it should be precomputed for numerical computation.

VII. DISCUSSION AND CONCLUDING REMARKS

Motivated by improving kinetic model equations for the kinetic methods such as a unified gas kinetic scheme and lattice Boltzmann method, this paper investigated the difference between the kinetic model equations and the fundamental Boltzmann equation in a kinetic regime. First, a shock wave structure case and a homogenous relaxation case are carried out to investigate these differences. The asymmetrical distribution and the velocity-dependent collision frequency are concluded to be the reasons for the deviations in the two cases, and limited success is achieved by using the information held by nonequilibrium moments and a velocity-dependent relaxation rate for adjusting the relaxation processes of kinetic model equations. After these comparisons, a relationship between the Boltzmann equation and the BGK equation are derived explicitly, where the Boltzmann collision term has been split into a BGK collision term and a residual. The BGK-based term represents the impacts of local, deviation and the residual represents the impacts of the global one. A generalized relaxation term is derived from this relation where the two factors for adjusting the model collision term are confirmed. After the analysis of the features of the deviation integral, which is an important part of the residual, an attempt at approximating the collision integral is also proposed in which the collision integral is approximated using simple patterns.

ACKNOWLEDGMENTS

The authors thank Professor Kun Xu for helpful discussions about gas kinetic theory. We would also like to thank reviewers for their constructive comments which significantly clarified the ideas in this comparison study. Sha Liu thanks Dr. Pubing Yu and Dr. Songze Chen at HKUST for discussions about the unified scheme. This project was financially supported mainly by the National High Technology Research and Development Program of China (Grant No. 2011AA7025042).

[1] S. Chapman and T. G. Cowling, *The Mathematical Theory of Nonuniform Gases: An Account of the Kinetic Theory of Viscosity, Thermal Conduction and Diffusion in Gases* (Cambridge University Press, Cambridge, 1991).
[2] C. Cercignani, *Rarefied Gas Dynamics: From Basic Concepts to Actual Calculations* (Cambridge University Press, Cambridge, 2000).
[3] P. Resibois and M. de Leener, *Classical Kinetic Theory of Fluids* (Wiley, New York, 1977).
[4] J. H. Ferziger and H. G. Kaper, *Mathematical Theory of Transport Processes in Gases* (North-Holland, Amsterdam, 1972).
[5] P. L. Bhatnagar, E. P. Gross, and M. Krook, Phys. Rev. **94**, 511 (1954).
[6] W. G. Vincenti and C. H. Krüger, *Introduction to Physical Gas Dynamics* (Krieger Pub Co, Malabar, Florida, 1975).
[7] K. Xu and J.-C. Huang, J. Comput. Phys. **229**, 7747 (2010).
[8] J. C. Huang, K. Xu, and P. B. Yu, Commun. Comput. Phys. **14**, 1147 (2013).
[9] S. Chen, K. Xu, C. Lee, and Q. Cai, J. Comput. Phys. **231**, 6643 (2012).
[10] X. Niu, C. Shu, and Y. Chew, Europhys. Lett. **67**, 600 (2004).
[11] S. Liu and C. Zhong, Phys. Rev. E **85**, 066705 (2012).
[12] J. W. Dufty, A. Santos, and J. J. Brey, Phys. Rev. Lett. **77**, 1270 (1996).
[13] L.-S. Luo, Phys. Rev. Lett. **81**, 1618 (1998).
[14] S. Chen and G. D. Doolen, Annu. Rev. Fluid Mech. **30**, 329 (1998).
[15] M. R. Swift, E. Orlandini, W. R. Osborn, and J. M. Yeomans, Phys. Rev. E **54**, 5041 (1996).
[16] X. Shan and H. Chen, Phys. Rev. E **47**, 1815 (1993).
[17] Y. S. Lian and K. Xu, J. Comput. Phys. **163**, 349 (2000).
[18] Q. Kang, D. Zhang, S. Chen, and X. He, Phys. Rev. E **65**, 036318 (2002).
[19] X. He, N. Li, and B. Goldstein, Mol. Simulat. **25**, 145 (2000).
[20] K. Yamamoto, X. He, and G. D. Doolen, J. Stat. Phys. **107**, 367 (2002).
[21] O. Filippova, S. Succi, F. Mazzocco, C. Arrighetti, G. Bella, and D. Hänel, J. Comput. Phys. **170**, 812 (2001).
[22] W. Liao, Y. Peng, and L.-S. Luo, Phys. Rev. E **80**, 046702 (2009).
[23] H. Yu, S. S. Girimaji, and L.-S. Luo, J. Comput. Phys. **209**, 599 (2005).
[24] Y.-H. Dong and P. Sagaut, Phys. Fluids **20**, 035105 (2008).
[25] J. Kerimo and S. S. Girimaji, J. Turbul. **8**, 1 (2007).
[26] G. A. Bird, *Molecular Gas Dynamics and the Direct Simulation of Gas Flows* (Clarendon Press, Oxford, 1994).
[27] G. A. Bird, NASA STI/Recon Technical Report A **76**, 40225 (1976).
[28] G. A. Bird, Phys. Fluids **13**, 2676 (1970).

[29] L. L. Baker and N. G. Hadjiconstantinou, Int. J. Num. Meth. Fl. **58**, 381 (2008).
[30] C. D. Landon and N. G. Hadjiconstantinou, *AIP Conf. Proc.* **1333**, 277 (2011).
[31] V. V. Aristov, *Direct Methods for Solving the Boltzmann Equation and Study of Nonequilibrium Flows*, Vol. 60 (Kluwer, Veröffentlicht, 2001).
[32] V. I. Kolobov, S. A. Bayyuk, R. R. Arslanbekov, V. V. Aristov, A. Frolova, and S. Zabelok, J. Spacecraft Rockets **42**, 598 (2005).
[33] V. I. Kolobov, R. R. Arslanbekov, V. Aristov, A. A. Frolova, and S. A. Zabelok, J. Comput. Phys. **223**, 589 (2007).
[34] A. B. Morris, P. L. Varghese, and D. B. Goldstein, J. Comput. Phys. **230**, 1265 (2011).
[35] C. D. Landon and N. G. Hadjiconstantinou, AIP Conf. Proc. **1333**, 277 (2011).
[36] Y. Sone, T. Ohwada, and K. Aoki, Phys. Fluids A **1**, 363 (1989).
[37] M. H. Ernst, Phys. Rep. **78**, 1 (1981).
[38] A. V. Bobylev, Dokl. Akad. Nauk SSSR **225**, 1296 (1975).
[39] M. Krook and T. T. Wu, Phys. Fluids **20**, 1589 (1977).
[40] D. Frenkel and M. H. Ernst, Phys. Rev. Lett. **63**, 2165 (1989).
[41] U. Frisch, B. Hasslacher, and Y. Pomeau, Phys. Rev. Lett. **56**, 1505 (1986).
[42] K. Xu and J.-C. Huang, IMA J. Appl. Math. **76**, 698 (2011).
[43] L. H. Holway Jr., Phys. Fluids **9**, 1658 (1966).
[44] E. M. Shakhov, Fluid Dyn. **3**, 95 (1968).
[45] L. Mieussens and H. Struchtrup, Phys. Fluids **16**, 2797 (2004).
[46] Y. Zheng and H. Struchtrup, Phys. Fluids **17**, 127103 (2005).
[47] P. Moxtov, H. Grad, and S. Borowitz, Phys. Rev. **90**, 376 (1953).
[48] C. K. Aidun and J. R. Clausen, Annu. Rev. Fluid Mech. **42**, 439 (2010).
[49] A. B. Morris, P. L. Varghese, D. B. Goldstein, AIP Conf. Proc. **1084**, 458 (2008).
[50] M. H. Ernst, Phys. Lett. A **69**, 390 (1979).
[51] H. M. Mott-Smith, Phys. Rev. **82**, 885 (1951).